Responses to reviewer 1: discussion (acp-2020-136)

October 9, 2020

The authors would like to thank Alexei Korolev for taking the time to review the manuscript and for his constructive feedback. We hope the responses provided below help to clarify the issues addressed. The adjustments made to the manuscript resulting from the feedback are summarized at the end of each response.

Remark by the authors In the original "referee comment", the reviewer is not referring to the latest version of the manuscript, but to the pre-discussion version. The line numbers and equation numbers have been adapted in the following to reflect the discussion paper.

1 Comments

R1-Co1. Since it was not specified in the text, it appears that Eq. 16 assumes that the lifetime of all hydrometeors is the same. This assumption would work well for riming particles falling through a mixed phase environment. However, the condition $T_p = 0°C$ will be limited by the freezing time of drops and should be accounted for in Eq. 16. Since freezing time for large and small drops may be different by few orders of magnitude (e.g. Murray and List, 1972), the effect of small droplets on the supersaturated volume may be lower than shown in Fig. 6. The following results obtained in this work will also be affected. The effect of freezing time for the case of freezing drops requires clarification.

The results of this work should be considered as a best-case scenario for ice enhancement, i.e. how much ice enhancement is to be expected at very favorable conditions. We agree with the reviewer that the assumption of $T_p = 0°C$ is more suitable for riming ice than for freezing drops, and it is now stated more clearly in the revised manuscript that riming ice is the main mechanism considered in this work.

When freezing drops are considered, $T_p = 0°C$ is still a good approximation for the surface temperature in case of inward freezing (Johnson and Hallett, 1968), however, unlike in the case of riming ice, there is no mechanism which sustains the gap in surface to ambient temperature after the freezing time is exceeded. The temperature distribution (for a given meteor size) will therefore not be concentrated on a single value, and instead, the rate at which new unfrozen droplets are available, the rate at which fully frozen droplets deplete and the size population dynamics with history effects have to be taken into account. Qualitatively, ice enhancement will be lower than the estimation given in the present work when the freezing time is taken into consideration. Because the freezing time is correlated positively to the meteor size, this deviation is expected to be more significant at low cloud temperatures, since the size distribution shifts towards lower values the lower the cloud temperature is. Therefore, freezing drops are even less likely to generate significant amounts of secondary ice than riming ice particles.

Adjustments to the manuscript: A sentence has been added (l.90/91) which clarifies that we are concerned with riming ice particles in this manuscript.

R1-Co2. The supersaturation calculation was considered for a particle free falling in still air, i.e. in a non- turbulent environment ($\epsilon = 0$). Could you speculate on a qualitative level, how $\epsilon > 0$ may affect your results? Would it increase or decrease the global ice

enhancement factor?
The study of Bagchi and Kottam (2008) is very helpful when the effect of ambient turbulence on the supersaturated volume and ice enhancement is discussed. The parameter range investigated in their work corresponds reasonably well to the scenario of a hydrometeor with a diameter of a few millimeter settling under atmospheric conditions, where the largest flow scales are expected to be $\mathcal{O}(100\text{m})$ and the smallest scales around $\mathcal{O}(1\text{mm})$ (Lehmann et al., 2009).

We know from simple mixing parcel models (e.g. (Chouippe et al., 2019, fig. 17) or (Prabhakaran et al., 2020, fig. 4)) that the highest supersaturations occur in regions where the temperature of the mixture is roughly halfway between T_∞ and T_p, i.e. $\tilde{T} \approx 0.5$ with $\tilde{T}$ being the non-dimensionalized temperature as introduced in the manuscript. In (Bagchi and Kottam, 2008, fig. 17) it is demonstrated that the centerline temperature in the wake decays significantly faster if the background flow is turbulent, especially when $\tilde{T} \lessapprox 0.4$. Therefore it is to be expected that supersaturation decays faster in the wake than it does for a uniform inflow, and thus, the supersaturated volume as well as the ice enhancement are most likely smaller if the ambient is turbulent.

However, Bagchi and Kottam (2008) also investigated the effect of turbulence on the heat and mass transfer coefficient. While the mean value of the Nusselt number remains mostly unaffected, strong fluctuations in its value can be observed. This presumably leads to a more intermittent behavior of the temperature and vapor fields. The role of intermittency on ice nucleation activity still needs to be investigated more thoroughly, especially when the distribution of aerosol particles is explicitly considered (a point which was suggested to be investigated as part of future work). If regions of strong supersaturation coincide with regions where AP are preferentially located, intermittency might promote ice nucleation as supersaturation and nucleation rate are non-linearly linked to the temperature/vapor fields.
Adjustments to the manuscript: A short discussion on the role of turbulence has been added in the conclusion section (l.418–423).
Note: This response is the same as the response to remark R2-Co2 raised by reviewer 2, due to the strong similarity of the remarks.

R1-Co3. What is the role of air pressure P on the results obtained in this paper (specifically Fig. 9)? Since particle fall speed, viscosity and thermal conductivity depend on P, it may have a noticeable effect on the mixing rate, supersaturated volume, amplitude of result supersaturation and the persistence of supersaturated regions. It is worth indicating what P was used in this study.
For the numerical simlations, no assumptions on the actual value of pressure have to be made since the incompressible Navier-Stokes equations are independent of the absolute value of pressure and the only imposed parameters in our framework are the particle Reynolds number, the Prandtl number and the Schmidt number, whose definitions are

$$Re = \frac{v_p D}{\nu},\ Pr = \frac{\nu}{D_T},\ Sc = \frac{\nu}{D_{n_v}}$$

where the dependency on the fluid density is approximately $\nu \sim \rho^{-1}$, $D_T \sim \rho^{-1}$ and $D_{n_v} \sim \rho^{-1}$ in the low density limit (see e.g. Bird et al. (2002)). Throughout this work, air is assumed to be an ideal gas and therefore

$$P \propto \rho T. \tag{1}$$

The only parameter affected by a variation in pressure is therefore the Reynolds number due to the modification in viscosity and fall speed of the hydrometeor. However, in the majority of the manuscript the dependency on the Reynolds number is neglected except for transitions in flow regimes. Therefore, the only relevant quantity within the framework of this work which is affected by the absolute value of pressure is the threshold diameter for regime transition (see response to R1-Co5 for the relationship). However, this quantity is already subject to various uncertainties such as the shape of the hydrometeor (affecting fall speed and flow regimes) and its density such that taking into account different pressure levels does not seem worthwhile. The supersaturated volume scaled by the hydrometeor volume is of

similar order of magnitude for both regimes investigated. Therefore, a shift in threshold diameter for transition alone is unable to lead to a significant alteration of the global ice enhancement factor.

In this work, the density of ambient air was assumed to be $1\,\mathrm{kg\,m^{-3}}$ which approximately corresponds to the values of atomospheric pressure presented in table 1 in the temperature range investigated according to the ideal gas equation of state.

temperature [°C]	−40	−30	−20	−10	0
pressure [kPa]	669	698	727	755	783

Table 1: Ambient air pressure for different air temperatures investigated.

R1-Co4. An important element not discussed in this study is the conceptual consideration of how this SIP process is related to natural clouds and identification of environmental conditions when it becomes significant. There are a few statements regarding this matter scattered throughout the manuscript. However, it leaves the reader with an impression of incompleteness of this paper. For example, as discussed in section 2, the condition $T_p = 0$°C can be satisfied for riming ice particle or freezing drops. For the first case, the accretion of cloud droplets on the ice surface should reach the wet growth regime, i.e. when LWC reach the Ludlam limit. At −30°C, for a free-falling hailstone, the Ludlam limit exceeds $5\mathrm{g\,m^{-3}}$ (the exact number needs to be checked). Such high LWC at −30°C does not seem to be feasible. Regarding the second case, there are very few reports on observations of precipitation size drops ($D > 100\mu$m) at −30°C. Therefore, this option also appears to be uncommon in clouds. In addition to the discussion on page 11 related to Fig. 9, it is worth expanding the discussion about the feasibility and significance of this SIP mechanism in temperatures warmer than −30°C. Mentioning that convective clouds are the most likely candidates for this type of SIP to occur would be also relevant.

The reviewer is correct that wet-growth at low cloud temperatures only occurs if the LWC is sufficiently high, and we arrive at a similar estimation for the Ludlam limit when applying the empirical formula of García-García and List (1992),

$$W_{f,SLL} = -2 \cdot 10^{-4} \frac{\mathrm{kg}}{\mathrm{m^3\,°C}} T_\infty, \tag{2}$$

which results in $W_{f,SLL} = 6\mathrm{g\,m^{-3}}$ for $T_\infty = -30$°C. Such high LWC and temperature gaps between the hydrometeors surface and the ambient exceed the range of values commonly observed in natural clouds, and merely served the purpose of demonstrating that exceptional/unrealistic conditions are required for this mechanism to be relevant. In accordance to the response given in R2-Ma1, we have decided to adjust the temperature range investigated and to focus on temperatures warmer than −15°C. The discussion on fig. 9 has been rewritten accordingly.

We also added a paragraph discussing the required cloud conditions to the manuscript, where the relevance of high LWC is emphasized. We agree that convective clouds are the most likely candidates for the required conditions.

Adjustments to the manuscript: The temperature range investigated has been adjusted. The text and figures in the manuscript have been adjusted accordingly. A paragraph discussing the required environmental conditions and possible cloud types in which they occur has been added to the manuscript (l.438–441).

R1-Co5. Eq.10: What $D_{j,min}$ and $D_{j,max}$ were used in this study? It is worth indicating the in the text.

The diameter thresholds were determined from the critical Reynolds numbers of regime transition Re_c

using the following set of equations.

$$Re_{c,j} = D_{j,max}|v_p|/\nu$$
$$v_p = u_g \left(3C_d(Re_{c,j})/4\right)^{-1/2}$$
$$u_g = \sqrt{\left(\rho_p/\rho_f - 1\right)|g|D_{j,max}}$$

The drag coefficient is approximated using the empirical drag law of Schiller and Naumann (1933). The density of the hailstone is assumed to be $600\mathrm{kg\,m^{-3}}$, as has been stated in the main text, and the fluid density was set to $1\mathrm{kg\,m^{-3}}$ (see also the response to R1-Co3 concerning this). Furthermore, the kinematic viscosity was set constant to $1 \cdot 10^{-5}\mathrm{m^2\,s^{-1}}$ in the discussion paper, but has been revised to a value of $1.68 \cdot 10^{-5}\mathrm{m^2\,s^{-1}}$ in the revised version of the manuscript, which corresponds approximately to the value at 750kPa air pressure and -10°C ambient temperature.

For Fig. 2 and Fig. 3 in the discussion paper, all four regimes are considered and the values of Re_c have been chosen in accordance to the values stated in section 3.1 of the discussion paper. The threshold diameters used in the discussion paper (D_{min}^{old}, D_{max}^{old}) and the revised manuscript (D_{min}^{new}, D_{max}^{new}) are summarized in table 2.

regime	D_{min}^{old}	D_{max}^{old}	D_{min}^{new}	D_{max}^{new}	Re_c
axisymmetric	0	0.77 mm	0	1.08 mm	212
steady oblique	0.77 mm	0.88 mm	1.08 mm	1.24 mm	273
oscillating oblique	0.88 mm	1.0 mm	1.24 mm	1.44 mm	360
chaotic	1.0 mm	∞	1.44 mm	∞	–

Table 2: Threshold diameters for regime transition used in the discussion paper (D_{min}^{old}, D_{max}^{old}) and the revised manuscript (D_{min}^{new}, D_{max}^{new}).

From section 3.2 onward, only the axisymmetric and chaotic regimes are considered and the following theshold diameter has been chosen for concreteness.

regime	D_{min}^{old}	D_{max}^{old}	D_{min}^{new}	D_{max}^{new}
axisymmetric	0	0.85 mm	0	1.26 mm
chaotic	0.85 mm	∞	1.26 mm	∞

Adjustments to the manuscript: Table 1 has been added to the manuscript which summarizes the threshold diameters. The adjusted threshold value used when only the axisymmetric and chaotic regimes are considered is stated in l.317.

R1-Co6. Definition of $\tilde{s}_i^*$ is worth introducing in the text prior to Fig.4.
Adjustments to the manuscript: The $\tilde{}$ notation has been removed from the manuscript.

R1-Co7. Line 222: Should it be $\tilde{s}_i^*$?
In this case, we are not referring to a threshold (as we do for the supersaturated volume), but to the supersaturation field itself, i.e. $\tilde{s}_i = \tilde{s}_i(\mathbf{x}, t)$. *Adjustments to the manuscript:* The expression has been rephrased as $s_i(\mathbf{x}, t) > s_{i,\infty}$ (l.227).

R1-Co8. Eq.16. Definitions of τ and Ω should be provided in the text.
We thank the reviewer for bringing this to our attention. Indeed the definitions of τ and Ω are absent in the text and will be added in the revised version of the manuscript. τ denotes the time over which the flow is time-averaged and Ω denotes the simulation domain, i.e. in this case a volume integral is computed over the entire domain of observation. *Adjustments to the manuscript:* The equation has been reformulated and τ has been omitted. The definition of Ω is given in l.232.

R1-Co9. Line 227: "... as a function of the threshold". I guess you employed $\tilde{s}_i^* = 0.1$ threshold. This should be indicated in the text.
This appears to be a misunderstanding. Eq. (16) in the discussion paper is an expression which computes the volume of fluid in the domain of observation which is supersaturated at a value higher than a given value (the threshold s_i^*), i.e. it answers the question "How much fluid volume exhibits a supersaturation of at least s_i^*?". In figure 6 of the discussion paper, the resulting volume is shown for varying thresholds, which are in the figure given as offsets from $s_{i,\infty}$. However, for reasons explained in the response to R2-Ma2, the supersaturated volume is given as a function of s_i^* instead of $\tilde{s}_i^* = s_i^* - s_{i,\infty}$ in the revised version of the manuscript (see fig. 6 of the revised manuscript).

R1-Co10. Lines 24 and 358: Field et al. 2016 should be 2017.
We thank the reviewer for pointing out this mistake, which has been corrected in the revised version of the manuscript.

References

Bagchi, P. and Kottam, K.: Effect of Freestream Isotropic Turbulence on Heat Transfer from a Sphere, Physics of Fluids, 20, 073 305, https://doi.org/10.1063/1.2963138, 2008.

Bird, R. B., Stewart, W. E., and Lightfoot, E. N.: Transport Phenomena, second edn., 2002.

Chouippe, A., Krayer, M., Uhlmann, M., Dušek, J., Kiselev, A., and Leisner, T.: Heat and Water Vapor Transfer in the Wake of a Falling Ice Sphere and Its Implication for Secondary Ice Formation in Clouds, New Journal of Physics, 21, 043 043, https://doi.org/10.1088/1367-2630/ab0a94, 2019.

García-García, F. and List, R.: Laboratory Measurements and Parameterizations of Supercooled Water Skin Temperatures and Bulk Properties of Gyrating Hailstones, Journal of the Atmospheric Sciences, 49, 2058–2073, https://doi.org/10.1175/1520-0469(1992)049⟨2058:LMAPOS⟩2.0.CO;2, 1992.

Johnson, D. A. and Hallett, J.: Freezing and Shattering of Supercooled Water Drops, Quarterly Journal of the Royal Meteorological Society, 94, 468–482, https://doi.org/10.1002/qj.49709440204, 1968.

Lehmann, K., Siebert, H., and Shaw, R. A.: Homogeneous and Inhomogeneous Mixing in Cumulus Clouds: Dependence on Local Turbulence Structure, Journal of the Atmospheric Sciences, 66, 3641–3659, https://doi.org/10.1175/2009JAS3012.1, 2009.

Prabhakaran, P., Kinney, G., Cantrell, W., Shaw, R. A., and Bodenschatz, E.: High Supersaturation in the Wake of Falling Hydrometeors: Implications for Cloud Invigoration and Ice Nucleation, Geophysical Research Letters, 47, e2020GL088 055, https://doi.org/10.1029/2020GL088055, 2020.

Schiller, L. and Naumann, A.: Über Die Grundlegenden Berechnungen Bei Der Schwerkraftaufbereitung, Z. Ver. Dtsch. Ing, 77, 318–320, 1933.

Responses to reviewer 2: discussion (acp-2020-136)

October 9, 2020

The authors would like to thank the anonymous referee for taking the time to review the manuscript and for addressing various important issues which helped us improving the quality of our work. We have decided to implement substantial changes to our manuscript based on his remarks, the details of which are addressed point by point below.

1 Major remarks

R2-Ma1. In the simulation, the surface temperature of the hydrometeor was fixed at 0°C. The ambient temperature was varied between −20°C and −40°C. Can the authors justify the choice of ambient temperatures for this study? Can the authors cite observations that detect wet growth at such low temperatures? There is a comprehensive experimental study by Greenan and List (JAS, 1995) on the surface temperature of hydrometeors at different conditions. It is unlikely that wet growth would occur at such low temperatures.

We agree with the reviewer that the temperature gap investigated in this work exceeds the range of values which are to be reasonably expected for natural clouds. The intention behind this was to demonstrate that extreme conditions are required in order to produce significant wake-induced ice enhancement, and that these conditions are unlikely to be observed in nature. However, this point apparently has not been communicated clearly enough. Furthermore, the decision to portray the contour plots at $T_\infty = -30°C$ seems unfortunate. We have therefore decided to vary the ambient temperature in a smaller range ($-15°C < T_\infty < 0°C$) according to the experimental observations by Greenan and List (1995) and depict the contours at $T_\infty = -15°C$.
Adjustments to the manuscript: The temperature range investigated has been adjusted. The text and figures in the manuscript have been adjusted accordingly.

R2-Ma2. In section 3.3 the authors define a parameter called ice enhancement factor to quantify the effects of enhanced supersaturation. This parameter is justified, but the expression used for finding NIN is not. This expression is used in Baker 1991, but none of the recent work on ice nucleation use this expression (to the best of reviewer's knowledge). Such a power law relationship between the number concentration of ice nuclei and supersaturation seems physically inconsistent. For example, barring the effects of wettability/chemical composition, as the supersaturation is increased, the size of the aerosols that is activated is reduced. For ice nucleation, the size of the nucleus is an important parameter, and as the size of the nucleus is reduced, its ice nucleating efficiency is also reduced. So, the number concentration of ice nuclei may not increase with supersaturation like a power law with such high exponents as mentioned in this paper. Furthermore, such a power law may not even be applicable to CCN concentrations when the supersaturation is quite high (Q. Ji and G. Shaw 1998 GRL). So, the applicability of such a power law to ice nuclei concentration is highly questionable. Can the authors comment/justify the applicability of the expression for NIN, as the whole of section 3.3 and the most important conclusion in the paper is based on this expression? This comment needs to be addressed in detail to support the conclusion. If this issue

cannot be addressed satisfactorily, the authors can consider presenting their arguments based on fractional cloud volume (like in section 3.2) that is exposed to the enhanced supersaturation due to the falling wet hydrometeors.
The power-law equation for N_{IN} indeed appears to be rarely used in recent literature. We have therefore decided to replace it by the exponential law provided by Meyers et al. (1992) which has been obtained from continuous-flow diffusion chamber (CFDC) measurements of natural aerosols. The constitutive relation is a parametrization of both the deposition and condensation-freezing mechanisms of ice nucleation and reads

$$N_{IN} = 0.528 \exp\left(12.96 s_i\right) \mathrm{m}^{-3}. \tag{1}$$

It is reported to be strictly valid for the following parameter range (the range of the CFDC data).

$$-20°\mathrm{C} < T < -7°\mathrm{C}, \quad 2\% < s_i < 25\%, \quad -5\% < s_w < 4.5\% \tag{2}$$

The temperatures of interest in the current work (after making the adjustments stated in R2-Ma1) fall well into the range of validity. The distribution of s_i in the wake is shown in fig. 6a (an updated version of fig. 6 of the discussion paper). For most ambient temperatures, s_i does not exceed 25%. At $T_\infty = -15°\mathrm{C}$, regions where s_i is slightly larger than 0.25 exist, but only occupy a small volume within the domain, and hence imprecisions are likely to be insignificant for integral quantities. When looking at the volumetric distribution of s_w in the wake in fig. 6b, it can be seen that water supersaturation exceeds the CFDC data range in significant portions of the domain when $T_\infty \lessapprox -10°\mathrm{C}$. Due to these relatively large supersaturations w.r.t. liquid, eq. (1) might underestimate the contribution of the condensation-freezing mode, as this mode shows increased activity under these conditions as has been demonstrated by Schaller and Fukuta (1979) for various substances. However, we are not aware of any parametrization of condensation-freezing nucleation for natural aerosols which can be directly applied under these conditions.

The main conclusion of this work is not affected by the substition of the nucleation law. The global ice enhancement factor computed with eq. (1) behaves similar to the power law estimation with $\alpha \approx 3$ as can be seen when comparing fig. 9 of the revised manuscript to fig. 9 of the discussion paper.
Adjustments to the manuscript: All affected figures have been updated and the text has been adjusted accordingly. Figure 6b has been added to the manuscript as it raises awareness concerning the applicability of eq. (1) and provides information on the supersaturation w.r.t. liquid which may be interesting for the reader. The choice and applicability of the consitutive relation is discussed in l.250–264.

R2-Ma3. The analysis in section 3.3 can be recast as the cloud volume that is exposed to very high supersaturation in the wake. This analysis concludes that the fraction of the cloud volume exposed to the high supersaturation in the wake is insignificant. There is a similar study published recently (Prabhakaran et al 2020 (GRL)). Their analysis concluded that a significant fraction of the cloud volume can be exposed to the high wake supersaturation during the lifetime of the cloud. Can the authors comment about the difference between these two analyses?
It is true that the current manuscript investigates the instanteneous exposure of a cloud subvolume to meteor-induced supersaturation, while the analysis presented in Prabhakaran et al. (2020) focuses on the volume swept by the meteors. The latter approach is reasonable since history effects in ice nucleation should be taken into account, i.e. it should be taken into account that ice nuclei which have been activated in the wake of a hydrometeor may stay activated once they are not exposed to the wake anymore. However, the difference in the two analyses can be regarded as two limiting cases of the nucleation rate, namely one which is limited by the rate of renewal of fluid in the wake (analysis of Prabhakaran et al. (2020)) and one which is limited by the time scale of nucleation (our analysis), as will be demonstrated in the following.

Following Prabhakaran et al. (2020), the time required for a significant volume of air to be sampled by hydrometeor wakes is estimated by

$$\tau_{sweep} = \left(\int_0^\infty \bar{N}_{met}(D) \dot{V}_{sweep}(D) \, \mathrm{d}D \right)^{-1}, \tag{3}$$

where $\bar{N}_{met}(D)$ denotes the number concentration density of ice particles and $\dot{V}_{sweep} = \epsilon v_p D^2 \pi/4$ is the volumetric flow rate of air which is swept by a hydrometeor with diameter D and velocity v_p. The unknown factor ϵ is assumed to be of the order of unity. Using eq. (10) of the discussion paper for $\bar{N}_{met}(D)$ and the terminal velocity for smooth spheres, we obtain $\tau_{sweep} \approx 110$s at $T = -15$°C, which fits the estimation of Prabhakaran et al. (2020) well. The use of an empirical law for the terminal velocity of frozen hydrometeors of natural shape leads to longer time scales, however, they are found to be of similar order of magnitude. This analysis tells us that even though the cloud volume which is instanteneously exposed to high supersaturations is very small, it does not take a long time to expose a significant volume because the rate at which air is swept by the meteors is high.

In the following we attempt to quantify the nucleation rate of INP, henceforth denoted as j_{met}, from our simulation data and the swept-volume argument. Under the assumption that nucleation occurs sufficiently fast to achieve the INP concentrations predicted by eq. (1), the nucleation rate can be estimated from the number of INP activated in the wake and the time it takes to replenish the volume of fluid affected by high supersaturations. The former is obtained directly from our simulation data by computing the volume integral $\int_{\Omega(D)} \left(N_{IN}(\mathbf{x}) - N_{IN,\infty}\right) \mathrm{d}\mathbf{x}$ while the latter is difficult to define objectively. We propose to estimate the time scale of wake renewal by

$$\tau_{expo} = \frac{V_{aff}}{\dot{V}_{sweep}} \tag{4}$$

where $V_{aff} = \gamma D^3 \pi/6$ is the volume affected by the wake of a hydrometeor of diameter D, which should be proportional to the volume of the hydrometeor. The prefactor γ is currently unknown, but might be related to the concept of supersaturated volume defined in the manuscript. The time scale τ_{expo} may be regarded as the characteristic time a fluid volume is exposed to high supersaturations, and hence the subscript. From the definitions of V_{aff} and $\dot{V}_{sweep}$ it follows that

$$\tau_{expo} \propto \frac{D}{v_p}, \tag{5}$$

with the constant of proportionality being referred to as C_{expo} hereafter. This new constant contains both unknown coefficients ϵ and γ and might be interpreted as the non-dimensional streamwise length of the wake. Again, this length is difficult to define rigorously due to the asymptotic decay of supersaturation. However, judging from fig. 7 it is likely that $C_{expo} = \mathcal{O}(10)$ which results in exposure times of the order of $\tau_{expo} \approx 5$ms for all diameters of interest. The swept-volume limited nucleation rate for an ensemble of meteors is then given by

$$j_{met}^{expo} = \int_0^\infty \bar{N}_{met}(D) \frac{1}{\tau_{expo}(D)} \int_{\Omega(D)} \left(N_{IN}(\mathbf{x}) - N_{IN,\infty}\right) \mathrm{d}\mathbf{x}\, \mathrm{d}D \tag{6}$$

under the assumptions that the rate of activation of INP is sufficiently fast, a sufficient number of interstitial aerosol particles are present and that those are homogeneously distributed within the wake.

The exposure time estimated previously is substantially shorter than the time scales usually relevant for cloud modelling (few milliseconds compared to minutes). As eq. (1) has been developed for cloud modelling, the validity of the assumption that INP activation can be regarded as instantaneous at the time scales considered should be brought into question. Indeed, classical nucleation theory (Fletcher, 1958) suggests that nucleation is a time-dependent process until the activated fraction of AP approaches unity. From concentrations of INP obtained from continuous-flow diffusion chamber (CFDC) experiments, the nucleation rate may be estimated by taking into account the residence time in the apparatus τ_{nucl} (Hoose and Möhler, 2012). Since eq. (1) is based on CFDC data, we make the conjecture that the local nucleation rate may be approximated by the relationship

$$j_{IN}(\mathbf{x}) \approx N_{IN}(\mathbf{x})/\tau_{nucl}. \tag{7}$$

In Hoose and Möhler (2012) residence times ranging from 1.6s to 120s are reported for various CFDC experiments. The primary data used to obtain eq. (1) also suggests that the peak concentration N_{IN} is achieved with residence times of approximately 10s (Al-Naimi and Saunders, 1985, fig. 6) and that

shorter residence times lead to lower concentrations (in accordance to the arguments stated before). As can already be seen, $\tau_{nucl} \gg \tau_{expo}$, and hence, the supposition that the INP concentrations predicted by eq. (1) are achieved within the exposure time is disproved. The rate-limited nucleation rate of the ensemble of hydrometeors is then given by

$$j_{met}^{nucl} = \int_0^\infty \bar{N}_{met}(D) \frac{1}{\tau_{nucl}} \int_{\Omega(D)} \left(N_{IN}(\mathbf{x}) - N_{IN,\infty} \right) \mathrm{d}\mathbf{x}\, \mathrm{d}D, \tag{8}$$

under the assumption that interstitial AP are entrained sufficiently fast into the wake (which is reasonable given the arguments by Prabhakaran et al. (2020)) and that they are distributed homogeneously within the wake.

Figure 10 shows the meteor-induced nucleation rate for both limiting cases. We assume that the most likely values for the tunable parameters are $C_{expo} = 10$ and $\tau_{nucl} = 10$s (solid lines), but also investigate the range $C_{expo} \in [1, 100]$ and $\tau_{nucl} \in [1, 100]$ s in order to pay regard to the uncertainties associated with these quantities (shaded area). The swept-volume limited estimation j_{met}^{expo} is at least two orders of magnitude higher than rate-limited estimation j_{met}^{nucl}. A high relevance of the wake-induced nucleation is indicated by j_{met}^{expo}, as it would only take around 40s for the number concentration of wake-activated INP to match the concentration of primary meteors at $T_\infty = -10$°C. In contrast, it would take around 82h to achieve this concentration with the rate-limited estimation, which suggests that this process is of little relevance in clouds. The large disparity between the results is explained by the differences in time scales, i.e. $\tau_{expo} = \mathcal{O}(10^{-3}\mathrm{s})$ while $\tau_{nucl} = \mathcal{O}(10^{1}\mathrm{s})$, as has been stated earlier. Physically this implies that the time a fluid volume is exposed to high supersaturations is too short to create considerable concentrations of INP.

This result can be linked to the ice enhancement factor introduced in the manuscript, as this quantity directly relates to the rate-limited estimation of the nucleation rate:

$$\langle f_i \rangle_{\mathcal{V}} = \frac{j_{met}^{nucl}}{N_{IN,\infty}/\tau_{nucl}} + 1. \tag{9}$$

Furthermore, it is straightforward to show that $\tau_{expo} \propto \tau_{sweep}$ for a given meteor concentration, which implies that as soon as a significant cloud volume is swept quickly at low volume fractions of ice, the transient exposure of a cloud fluid element to the wake will be short.

In order for wake-induced ice nucleation to be a relevant SIP, the nucleation rate in the wake needs to be significantly higher than what has been estimated in this work. If the conjectures presented in the above analysis hold, the most feasible way to accomplish this is that the overall concentration of AP is higher than what has been assumed in this work implicitly through eq. (1), i.e. this mechanism may gain importance in clouds with a high number of possible nucleation sites. It might also be conceivable that the AP concentration is locally enhanced in the wake due to flow-induced clustering, i.e. AP may be preferentially located in highly supersaturated region as opposed to the ambient, although this mechanism unlikely leads to the required concentrations. Nonetheless, we suggest that an analysis of individual AP trajectories may be beneficial in the future to clarify the importance of this SIP, as such an analysis would allow for a more rigorous assessment of the nucleation rate by providing access to the actual residence times of AP and by enabling the use of more fundamental constitutive laws for ice nucleation (such as classical nucleation theory).

Adjustments to the manuscript: Subsection 3.3 has been revised and partially reformulated. Subsection 3.4 has been added to the manuscript, which discusses the difference in the two analyses. Figure 10 has been added to the manuscript. The notation regarding the concentration density of primary hydrometeors has been adjusted (l.170).

2 Comments

R2-Co1. In lines 108-109, the authors state that buoyancy contributions to momentum due to the variations in temperature and water vapor is negligible. Can the authors justify this statement briefly (a few lines) by quoting the value of the relevant parameter, e.g. Richardson number, along with the reference to Chouippe et al 2019? Would it be

insignificant when the temperature difference between the ambient and the drop is 40°C**? Similarly, in lines 118-119, can the authors justify briefly why the variations in the vertical velocity is not important in the present context?**
The Richardson number for a freely falling heated sphere has been defined in Chouippe et al. (2019) as

$$Ri_T = \frac{1}{\left(\frac{\rho_p}{\rho_\infty} - 1\right)} \frac{T_p - T_\infty}{T_\infty}, \tag{10}$$

where T_∞ is given in Kelvin (see (Chouippe et al., 2019, Appendix A) for the derivation). In accordance to the value stated in the discussion paper, we assume $\rho_p = 600\text{kg}\,\text{m}^{-3}$ and $\rho_\infty = 1\text{kg}\,\text{m}^{-3}$. For an ambient temperature of $T_\infty = -40°\text{C} = 233.15\text{K}$ and a particle temperature of $T_\infty = 0°\text{C} = 273.15\text{K}$, we obtain

$$Ri_T \approx 3 \cdot 10^{-4}. \tag{11}$$

In (Chouippe et al., 2019, fig. 7) it is documented that the recirculation length of the wake, a quantity which is shown to be sensitive to buoyancy effects, does not differ significantly from passive scalar transport when $Ri_T = 1 \cdot 10^{-3}$, which is a value significantly higher than what is investigated in the present manuscript.

The Richardson number due to variations in water vapor content is defined as

$$Ri_{n_v} = -\frac{1}{\left(\frac{\rho_p}{\rho_\infty} - 1\right)} \frac{M_w - M_d}{N_a \rho_\infty} (n_{v,p} - n_{v,\infty}), \tag{12}$$

where N_A is the Avogadro constant, M_w the molar mass of water and M_d the mixture molar mass of dry air (Chouippe et al., 2019, eq. (45)). Using the temperatures stated in the previous paragraph and the vapor boundary conditions stated in the manuscript, we obtain

$$Ri_{n_v} \approx 5 \cdot 10^{-6}, \tag{13}$$

which is orders of magnitudes smaller than Ri_T. Please note that eq. (4) in the discussion paper is incorrect and should read

$$n_v = e/k_b T. \tag{14}$$

This has been corrected in the revised version of the manuscript.

Fluctuations in $\mathbf{v}_p$ are only important in the context of this manuscript if they lead to modifications in the structure of the wake. The equations of motion for the spherical particle suggest that the time scale of particle acceleration is proportional to ρ_p/ρ_∞ (Chouippe et al., 2019, eq. (8)). If this time scale is much larger than the observation time of interest, which in our case is L_x/v_p with L_x being the length of the simulation domain, the wake will have a structure similar to that of particle falling through a fluid at rest with constant velocity. In other words the structure of the wake is only altered if the particle changes its falling direction significantly during the observation time. In (Chouippe et al., 2019, § 3.3) it is reported that a freely falling particle with $\rho_p/\rho_\infty = 10$ already behaves very similar to a fixed particle ($\rho_p/\rho_\infty \to \infty$) e.g. in terms of centerline temperature evolution and half-width of the thermal wake. Since we assume a much larger density ratio of 600, it seems unlikely that fluctuations in particle velocity have an impact on the shape of the wake.
Adjustments to the manuscript: Equation (4) has been corrected. A half-sentence stating that the wake of a freely falling hydrometeor behaves similar to that of a fixed particle due to the high value of the density ratio has been added (l.124).

R2-Co2. In a deep convective cloud, the hydrometeors are falling through a turbulent environment. Can the authors comment about the role of turbulent fluctuations in the ambient? How would the volume of the supersaturated region change with turbulence intensity in the ambient? There are some heat transfer studies from a heated sphere in a turbulent environment (Bagchi and Kottam 2008, Phys of Fluids). Can this be extended to the current study? It might be worthwhile to briefly discuss this as a part of future

work.
The study of Bagchi and Kottam (2008) is very helpful when the effect of ambient turbulence on the supersaturated volume and ice enhancement is discussed. The parameter range investigated in their work corresponds reasonably well to the scenario of a hydrometeor with a diameter of a few millimeter settling under atmospheric conditions, where the largest flow scales are expected to be $\mathcal{O}$(100m) and the smallest scales around $\mathcal{O}$(1mm) (Lehmann et al., 2009).

We know from simple mixing parcel models (e.g. (Chouippe et al., 2019, fig. 17) or (Prabhakaran et al., 2020, fig. 4)) that the highest supersaturations occur in regions where the temperature of the mixture is roughly halfway between T_∞ and T_p, i.e. $\tilde{T} \approx 0.5$ with $\tilde{T}$ being the non-dimensionalized temperature as introduced in the manuscript. In (Bagchi and Kottam, 2008, fig. 17) it is demonstrated that the centerline temperature in the wake decays significantly faster if the background flow is turbulent, especially when $\tilde{T} \lessapprox 0.4$. Therefore it is to be expected that supersaturation decays faster in the wake than it does for a uniform inflow, and thus, the supersaturated volume as well as the ice enhancement are most likely smaller if the ambient is turbulent.

However, Bagchi and Kottam (2008) also investigated the effect of turbulence on the heat and mass transfer coefficient. While the mean value of the Nusselt number remains mostly unaffected, strong fluctuations in its value can be observed. This presumably leads to a more intermittent behavior of the temperature and vapor fields. The role of intermittency on ice nucleation activity still needs to be investigated more thoroughly, especially when the distribution of aerosol particles is explicitly considered (a point which was suggested to be investigated as part of future work). If regions of strong supersaturation conincide with regions where AP are preferentially located, intermittency might promote ice nucleation as supersaturation and nucleation rate are non-linearly linked to the temperature/vapor fields.
Adjustments to the manuscript: A short discussion on the role of turbulence has been added in the conclusion section (l.418–423).
Note: This response is the same as the response to remark R1-Co2 raised by Alexei Korolev, due to the strong similarity of the remarks.

R2-Co3. Can the authors comment on how the supersaturated volume would be affected in the presence of cloud droplets and ice particles in the ambient?
If a second riming ice particle or warm droplet approaches the settling ice particles, their thermal/vapor wakes will interact, which probably leads to reduced heat and mass transfer as temperature/vapor gradients are dampened in the boundary layer. Therefore the supersaturated volume induced by two nearby hydrometeors is likely to be smaller than their sum.

If a cloud droplet or ice particle which is colder than the riming meteor enters the wake, e.g. a hydrometeor at ambient temperature, water vapor may be removed from the gas phase by diffusional growth of the secondary hydrometeor. This presumably leads to a depletion of supersaturation, and hence, the supersaturated volume decreases.

3 Minor remarks

R2-Mi1. Excess supersaturation - notation difference between Eq. 15 and Fig 4 caption. Fig 4 caption has a "*" on top of "s".
We thank the reviewer for pointing out this mistake.
Adjustments to the manuscript: The caption has been adjusted.

References

Al-Naimi, R. and Saunders, C. P. R.: Measurements of Natural Deposition and Condensation-Freezing Ice Nuclei with a Continuous Flow Chamber, Atmospheric Environment (1967), 19, 1871–1882, https://doi.org/10.1016/0004-6981(85)90012-5, 1985.

Bagchi, P. and Kottam, K.: Effect of Freestream Isotropic Turbulence on Heat Transfer from a Sphere, Physics of Fluids, 20, 073 305, https://doi.org/10.1063/1.2963138, 2008.

Chouippe, A., Krayer, M., Uhlmann, M., Dušek, J., Kiselev, A., and Leisner, T.: Heat and Water Vapor Transfer in the Wake of a Falling Ice Sphere and Its Implication for Secondary Ice Formation in Clouds, New Journal of Physics, 21, 043 043, https://doi.org/10.1088/1367-2630/ab0a94, 2019.

Fletcher, N. H.: Size Effect in Heterogeneous Nucleation, The Journal of Chemical Physics, 29, 572–576, https://doi.org/10.1063/1.1744540, 1958.

Greenan, B. J. W. and List, R.: Experimental Closure of the Heat and Mass Transfer Theory of Spheroidal Hailstones, Journal of the Atmospheric Sciences, 52, 3797–3815, https://doi.org/10.1175/1520-0469(1995)052⟨3797:ECOTHA⟩2.0.CO;2, 1995.

Hoose, C. and Möhler, O.: Heterogeneous Ice Nucleation on Atmospheric Aerosols: A Review of Results from Laboratory Experiments, Atmospheric Chemistry and Physics, 12, 9817–9854, https://doi.org/10.5194/acp-12-9817-2012, 2012.

Lehmann, K., Siebert, H., and Shaw, R. A.: Homogeneous and Inhomogeneous Mixing in Cumulus Clouds: Dependence on Local Turbulence Structure, Journal of the Atmospheric Sciences, 66, 3641–3659, https://doi.org/10.1175/2009JAS3012.1, 2009.

Meyers, M. P., DeMott, P. J., and Cotton, W. R.: New Primary Ice-Nucleation Parameterizations in an Explicit Cloud Model, Journal of Applied Meteorology, 31, 708–721, https://doi.org/10.1175/1520-0450(1992)031⟨0708:NPINPI⟩2.0.CO;2, 1992.

Prabhakaran, P., Kinney, G., Cantrell, W., Shaw, R. A., and Bodenschatz, E.: High Supersaturation in the Wake of Falling Hydrometeors: Implications for Cloud Invigoration and Ice Nucleation, Geophysical Research Letters, 47, e2020GL088 055, https://doi.org/10.1029/2020GL088055, 2020.

Schaller, R. C. and Fukuta, N.: Ice Nucleation by Aerosol Particles: Experimental Studies Using a Wedge-Shaped Ice Thermal Diffusion Chamber, Journal of the Atmospheric Sciences, 36, 1788–1802, https://doi.org/10.1175/1520-0469(1979)036⟨1788:INBAPE⟩2.0.CO;2, 1979.

On the ice-nucleating potential of warm hydrometeors in mixed-phase clouds

Michael Krayer[1], Agathe Chouippe[1,a], Markus Uhlmann[1], Jan Dušek[2], and Thomas Leisner[3]

[1]Institute for Hydromechanics, Karlsruhe Institute of Technology (KIT), Karlsruhe, Germany
[2]ICube, Fluid Mechanics Group, Université de Strasbourg, Strasbourg, France
[3]Institute of Meteorology and Climate Research, Atmospheric Aerosol Research Department, Karlsruhe Institute of Technology (KIT), Eggenstein-Leopoldshafen, Germany
[a]now at: ICube, Fluid Mechanics Group, Université de Strasbourg, Strasbourg, France

Correspondence: Michael Krayer (michael.krayer@kit.edu)

Abstract. The question whether or not the presence of warm hydrometeors in clouds may play a significant role in the nucleation of new ice particles has been debated for several decades. While the early works of Fukuta and Lee (1986) and Baker (1991) indicated that it might be irrelevant, the more recent study of ~~Prabhakaran et al. (2019)~~ Prabhakaran et al. (2020) suggested otherwise. In this work, we ~~are aiming~~ attempt to quantify the ice-nucleating potential using high-fidelity flow simulation techniques around a single hydrometeor and use favorable considerations to upscale the effects to a collective of ice particles in clouds. While we find that ice nucleation may be significantly enhanced in the vicinity of a warm hydrometeor ~~by several orders of magnitude~~ and that the affected volume of air is much larger than previously estimated, it is ~~very~~ unlikely that this effect alone causes the rapid enhancement of ice nucleation observed in some types of clouds, mainly due to the low initial volumetric ice concentration. ~~Nonetheless~~Furthermore, it is ~~suggested to implement this effect~~ demonstrated that the excess nucleation rate does not primarily depend on the rate at which cloud volume is sampled by the meteors' wakes, but is rather limited by the exposure time of ice nucleating particles to the wake, which is estimated to be of the order of few microseconds. It is suggested to further investigate this phenomenon by tracking the trajectories of ice nucleating particles in order to obtain a parametrization which can be implemented into existing cloud models ~~in order~~ to investigate second-order effects such as ice ~~nucleus preactivation or~~ enhancement after the onset of glaciation.

1 Introduction

The formation of hydrometeors in clouds is of great importance for the prediction of weather and cloud electrification, as well as for the hydrological cycle, and thus, eventually for the evolution of climate. However, despite its relevance and great research effort over the past decades, many aspects remain poorly understood. One such puzzle is the discrepancy between the concentration of ice particles and that of available ice nuclei (IN) in airborne observations by several orders of magnitude (Pruppacher and Klett, 2010) which has been observed for various cloud types (Koenig, 1963; Auer et al., 1969; Hobbs, 1969; Hobbs and Rangno, 1985; Mossop, 1985; Hogan et al., 2002). This phenomenon has been termed *ice enhancement* and various

mechanisms which amplify primary ice nucleation have been proposed to explain the observed surplus in ice particles ~~(?)~~ (Field et al., 2017) .

The most promising class of enhancement mechanisms is the so-called *secondary ice production* (SIP), where new ice is formed from preexisting ice particles. Commonly accepted SIP include rime-splintering (Hallett and Mossop, 1974), fragmentation of ice (Vardiman, 1978; Takahashi et al., 1995; Bacon et al., 1998) and freezing drops (Hobbs and Alkezweeny, 1968). Most of these mechanisms have been implemented into cloud models with explicit ice microphysics (see ~~?~~ Field et al. (2017) for a recent overview), which, however, are not capable of satisfactorily explaining the large amount of ice particles in observations. Further mechanisms have been proposed in the past whose relative importance is still to be evaluated.

While studying the effect of supersaturation on primary ice formation, Gagin (1972) proposed several mechanisms which locally produce high values of supersaturation, and thus, regions of significantly enhanced nucleation activity. He suggested that freezing hydrometeors, which attain higher temperatures than the surrounding air due to the release of latent heat, may cause transient supersaturation by ~~simulateneous~~ simultaneous evaporation and heat transfer and linked it to the observation of satellite drops which have previously been observed experimentally during the freezing of supercooled droplets by Dye and Hobbs (1968). This hypothesis was corroborated by Nix and Fukuta (1974), who investigated numerically the transient freezing process of an isolated droplet.

Another phenomenon which leads to localized supersaturation around hydrometeors is the riming process of ice particles in mixed-phase clouds with high liquid-water content (Gagin, 1972). Here, sufficiently large ice particles collect supercooled droplets from their surroundings, which then accumulate on its surface and subsequently freeze, leading to similar non-equilibrium conditions as observed for the freezing drop. The supersaturation around a riming ice particle has been investigated numerically by Fukuta and Lee (1986) assuming steady conditions. Indeed, they found that the air in the vicinity of a warm ice particle can be highly supersaturated, while the magnitude and spatial extent strongly increase with increasing difference in surface to ambient temperature. However, even at low cloud temperatures, the supersaturated regions do not extend far away from the hydrometeor in their simulations, which led to the conclusion of Rangno and Hobbs (1991) that the overall ice enhancement is likely to be negligible.

While the previously mentioned studies focused on the quantification of the supersaturation field, Baker (1991) attempted to quantify the actual effect on ice enhancement around warm hydrometeors. He concluded that, although significant ice enhancement factors appear to be possible, the affected air mass seems to be too small to substantially contribute to the explanation of the discrepancy between ice crystal and ice nucleus concentrations.

Recently, the potential of hail and rain to nucleate droplets has gained new attention when Prabhakaran et al. (2017) observed condensation in the wake of cold droplets in a moist convection apparatus. In their experiment, a pressurized mixture of sulfur hexafluoride/helium was used and operating conditions were chosen such that slight supersaturations led to homogeneous condensation, which could indeed be observed in the wake of larger falling droplets. However, their results can only be qualitatively ~~transfered~~ transferred to Earth's atmosphere mainly due to the difference in primary nucleation mechanism. Moreover, the mechanism to create supersaturation is different from the previously discussed one in the sense that the droplets are colder than the surrounding air.

To overcome these shortcomings, ~~Prabhakaran et al. (2019)~~ Prabhakaran et al. (2020) conducted a similar laboratory experiment using moist air which has been seeded with aerosol particles (AP) as an operating medium to investigate heterogeneous nucleation in the wake of a warm falling droplet. Again, significant nucleation was observed in the wake of the falling hydrometeor. While the extent of wake-induced nucleation has not been quantified, the affected volume of air appears to be significantly larger than the predictions of Fukuta and Lee (1986) and Baker (1991) were suggesting. This discrepancy might be related to the strong assumptions on the flow made in these early works, which neglect important features of the wake of falling objects that are nowadays accessible to numerical simulations (Johnson and Patel, 1999; Bouchet et al., 2006; Zhou and Dušek, 2015). In particular, it has been shown that both unsteadiness and vortical structures of the flow strongly affect the temperature and vapor concentration in the vicinity and far downstream of a falling sphere (Bagchi et al., 2001; de Stadler et al., 2014), and thus strongly affect the distribution of supersaturation around hydrometeors (Chouippe et al., 2019).

In Chouippe et al. (2019), we presented a framework for high-fidelity numerical simulations of heat and mass transfer around a falling ice particle which is not in thermal equilibrium with its surroundings. Even though the focus was predominantly set towards several methodological questions, it was shown qualitatively that the local supersaturation differs strongly from the simpler considerations of Fukuta and Lee (1986).

The present work aims to revisit the details of the supersaturation field around an idealized falling hydrometeor and to quantify the volume of air which is affected by the presence of hydrometeors. Furthermore, it is yet to be evaluated how significant meteor-induced enhancement of ice nucleation is in clouds (Korolev et al., 2020), and therefore, we attempt to link our results to heterogeneous nucleation of aerosol particles.

2 Methodology

In order to assess the spatial structure of supersaturation around hydrometeors, knowledge on the flow around it is essential. This is not an easy task, since the features of the flow may strongly depend on parameters such as the size, shape and surface properties of the hydrometeor, which typically vary substantially, especially if ice particles are concerned.

In this work we utilize the numerical framework previously presented in Chouippe et al. (2019) and model the hydrometeor as a sphere with constant diameter D, constant surface temperature T_p and a constant vapor pressure $e_{v,p}$ at its surface. The latter is determined by the assumption of local equilibrium at the surface, and thus, corresponds to the saturation vapor pressure $e_{sat,j}$ at T_p. Here, j denotes the phase of water on the surface of the hydrometeor, where subscript "i" (ice) will be used to denote the solid phase and "w" (water) to denote the liquid phase.

The boundary conditions for the heat and mass transfer problem are motivated by the conditions expected for riming ice particles in the wet-growth regime (Ludlam limit). A surface temperature of $T_p = 0\,^{\circ}\mathrm{C}$ is assumed, i.e. the surface of the ice sphere is warmer than the local cloud temperature, since the latter is generally below the freezing point in mixed-phase clouds. Please note that at this surface temperature the equilibrium vapor pressure with respect to both the liquid and solid phase coincide, and hence, no assumptions on the phase at the surface have to be made. Since the actual riming process is not modelled explicitly, but only enters through the boundary conditions of the heat and mass transfer problem, the results of this

work are more general and can in principle be applied to any configuration which contains a mechanism leading to a warm hydrometeor, such as a freezing droplet or rapid decreases in cloud temperature. Nonetheless, riming ice particles are likely the most relevant application, since the riming mechanism allows for a temperature gap which is sustained and not transient.

One of the key parameters for the investigation of wake-induced ice nucleation is the distribution of the saturation ratio

$$S_j(e,T) = e/e_{sat,j}(T), \tag{1}$$

where e denotes the local vapor pressure. A parametrization of $e_{sat,j}$ with respect to temperature for both phase equilibria in the temperature range of interest is adopted from Murphy and Koop (2005). The spatial distribution of S_j can then be reconstructed from the temperature field T and the vapor concentration n_v, which are governed by the transport equations

$$\frac{\partial T}{\partial t} + \boldsymbol{u}\cdot\boldsymbol{\nabla}T = \mathcal{D}_T\boldsymbol{\nabla}^2 T, \tag{2}$$

$$\frac{\partial n_v}{\partial t} + \boldsymbol{u}\cdot\boldsymbol{\nabla}n_v = \mathcal{D}_{n_v}\boldsymbol{\nabla}^2 n_v, \tag{3}$$

where $\mathcal{D}_T$ and $\mathcal{D}_{n_v}$ denote the heat and vapor diffusivities and $\boldsymbol{u} = (u,v,w)^T$ is the velocity field of the surrounding air. The partial pressure of water is linked to these transported quantities by

$e = n_v/k_b T,$

$$e = n_v k_b T, \tag{4}$$

where k_b is Boltzmann's constant. Even though the diffusivities of both vapor and heat are similar in magnitude, it was shown by Chouippe et al. (2019) that assuming equal diffusivities leads to an underestimation of the saturation ratio, and hence, both equations will be treated separately.

Under the boundary conditions described earlier, Eq. (2) leads to an outward heat flux, because the surface temperature of the hydrometeor is higher than that of its surrounding. Furthermore, at $T_p = 0\,^\circ\mathrm{C}$ the vapor concentration at the meteor's surface is generally higher than in the ambient, since the latter is assumed to be in equilibrium with the liquid phase at the corresponding cloud temperature $T_\infty < T_p$ due to the presence of droplets in mixed-phase clouds, i.e. $e_\infty = e_{sat,w}(T_\infty)$. This results in an outward vapor flux, and hence, the hydrometeor will also evaporate. It is therefore of primary importance to resolve the temporal and spatial variations of both temperature and concentration fields.

In Chouippe et al. (2019) we have shown that buoyant forces due to density variations within the fluid phase caused by variations in temperature and concentration are negligible at the parameter point of interest. The flow can then be approximated by the incompressible Navier-Stokes equations,

$$\boldsymbol{\nabla}\cdot\boldsymbol{u} = 0, \tag{5}$$

$$\frac{\partial \boldsymbol{u}}{\partial t} + (\boldsymbol{u}\cdot\boldsymbol{\nabla})\boldsymbol{u} = -\frac{1}{\rho_f}\boldsymbol{\nabla}p + \nu\boldsymbol{\nabla}^2\boldsymbol{u}, \tag{6}$$

where p denotes the hydrodynamic pressure, ρ_f the density and ν the kinematic viscosity of the fluid. The flow is driven by the falling motion of the hydrometer, which is assumed to be moving with a constant velocity $\boldsymbol{v}_p$ equal to its terminal velocity v_T, i.e.

$$\boldsymbol{v}_p = -v_T \boldsymbol{e}_z, \tag{7}$$

where $\boldsymbol{e}_z$ is the unit vector in the z-direction. The fluid ahead of the hydrometeor is assumed to be at rest. This setup is equivalent to a system with a fixed sphere positioned in an upcoming flow, which differs from that of a freely falling mobile sphere in the sense that fluctuations in $\boldsymbol{v}_p$ are not permitted. The necessity to account for these variations has been discussed in Chouippe et al. (2019) and it was found that it has little influence in the present context due to the expected high value of the density ratio.

The Navier-Stokes and scalar transport equations are solved numerically in non-dimensional form. In particular lengths are scaled by the particle diameter D, velocity components by the terminal velocity v_T and the scalar transport equations are formulated in terms of

$$\tilde{T} = (T - T_\infty)/(T_p - T_\infty), \tag{8}$$

$$\tilde{n}_v = (n_v - n_{v,\infty})/(n_{v,p} - n_{v,\infty}), \tag{9}$$

which has the advantage, that various dimensional boundary conditions, e.g. various values of T_∞, can be studied in post-processing from a single simulation run. Under the simplifications stated, the non-dimensional problem can be parametrized by the Reynolds number, $Re = |\boldsymbol{v}_p| D/\nu$, the Prandtl number, $Pr = \nu/\mathcal{D}_T$, and the Schmidt number, $Sc = \nu/\mathcal{D}_{n_v}$. While the Reynolds number is varied up to a value of $Re = 600$, the Prandtl and Schmidt numbers are set, respectively, to values of $Pr = 0.72$ and $Sc = 0.63$ in this study, which correspond to representative values expected for humid air in the temperature range of interest.

The numerical method employed is based on the method of Jenny and Dušek (2004), which has been used by e.g. Kotouč et al. (2008) and Chouippe et al. (2019) to simulate heat and mass transfer around spherical particles. It relies on a spectral/spectral-element discretiztion of the Navier-Stokes equations (Eq. 5,6) coupled to the transport of heat and mass (Eq. 2,3). The spherical particle is placed at the origin of a cylindrical domain Ω. On the surface of the particle impermeability and no-slip boundary conditions are imposed, while the scalar fields are subject to the constant Dirichlet boundary conditions $\tilde{T} = \tilde{n}_v = 1$. At the upstream boundary of the simulation domain, a uniform velocity condition and $\tilde{T} = \tilde{n}_v = 0$ are enforced, while the downstream boundary is subject to zero-gradient boundary conditions for velocity as well as the scalars. The lateral boundaries are stress-free with zero-gradient boundary conditions for the scalars and zero pressure is imposed. The axial-radial plane is decomposed using the spectral element method of Patera (1984), while the homogeneous azimuthal direction is treated using Fourier decomposition. The numerical mesh used in this work is shown in fig. 1. For the temporal integration a time splitting method is used which consists of an explicit third order Adams-Bashforth discretization for the advective terms and a first order fully implicit discretization of the diffusion terms (Rønquist, 1988).

In the vertical direction the domain has a total length of $62D$, where the inflow length is $12D$ and the outflow length $50D$ measured from the center of the sphere. The diameter of the domain is $16D$. The computational domain has therefore been extended in the rear of the sphere compared to our former simulations presented in Chouippe et al. (2019). In total, 463 two-dimensional elements, each containing $[6 \times 6]$ collocation points, have been distributed over the domain. The azimuthal Fourier series is truncated at the 7th mode. This resolution is comparable to our previous work and has been shown to give good results for the momentum, as well has heat and mass transfer. All relevant scales of the flow and the scalar fields are resolved.

For more details on the numerical framework, the reader is referred to the previous work of Chouippe et al. (2019).

3 Results

3.1 Hydrometeor wake regimes in clouds

The dynamics of the flow around spherical objects are, under the assumptions stated in the previous section, fully parametrized by the Reynolds number, which depends on the diameter and indirectly, through modulation of the terminal velocity, on the density of the hydrometeor. Depending on the Reynolds number value, various flow states emerge in the wake (Johnson and Patel, 1999; Jenny et al., 2004; Kotouč et al., 2009). At low values the wake is axisymmetric and steady. When the first critical value of the Reynolds number, $Re_{c,1} \approx 212$, is exceeded, the wake becomes oblique with respect to the falling direction (*steady oblique regime)* and only planar symmetry may be observed (Ghidersa and Dušek, 2000). At $Re_{c,2} \approx 273$ a second instability of Hopf type occurs (Ghidersa and Dušek, 2000), which leads to unsteady periodic vortex shedding, while planar symmetry is still maintained (*oscillating oblique regime*). Eventually the vortex shedding becomes chaotic at $Re_{c,3} \approx 360$ (Ormières and Provansal, 1999) and all instantaneous symmetries are lost (*chaotic regime*). The listed regimes differ significantly in their ability to transfer heat and mass (Chouippe et al., 2019), and thus, different characteristics in producing local supersaturation are to be expected.

In order to estimate the distribution of ice particle wake regimes in clouds, we adopt the size distribution of Marshall and Palmer (1948),

$$N = N_0 \exp(-\lambda D),$$

$$\bar{N}_{met} = \bar{N}_{met,0} \exp(-\lambda D), \tag{10}$$

where ~~N~~ $\bar{N}_{met}$ is the number concentration density of hydrometeors per unit volume of air and ~~N_0, λ~~ $\bar{N}_{met,0}, \lambda$ are model parameters. Equation (10) has originally been developed for raindrops, however, its validity for sufficiently large ice particles has been demonstrated by Passarelli (1978); Houze et al. (1979); Gordon and Marwitz (1984); Herzegh and Hobbs (1985); Patade et al. (2015) for various types of natural clouds. The values of the model parameters ~~N_0, λ~~ $\bar{N}_{met,0}, \lambda$ are usually obtained by airborne measurements and given as functions of the cloud temperature. One such parametrization is provided by

Houze et al. (1979) for frontal clouds within a temperature range from $-42°\mathrm{C}$ to $+6°\mathrm{C}$, which will be used in the following for the size distribution of primary ice and is given by the constitutive equations

$$N_0(T) = 5.5 \cdot 10^6 \exp(-0.09T)\,\mathrm{m}^{-4},$$
$$\lambda(T) = 9.6 \cdot 10^{-1} \exp(-0.056T)\,\mathrm{mm}^{-1},$$

$$\bar{N}_{met,0}(T) = 5.5 \cdot 10^6 \exp(-0.09T)\,\mathrm{m}^{-4}, \tag{11}$$
$$\lambda(T) = 9.6 \cdot 10^{-1} \exp(-0.056T)\,\mathrm{mm}^{-1}, \tag{12}$$

where T denotes the cloud temperature in °C. For this cloud type, ice enhancement has been previously reported in the presence of riming ice particles (Hogan et al., 2002). Even though it is known that the number density of ice particles of sub-millimeter size might deviate significantly from Eq. (10) in a sub-exponential or super-exponential manner (Passarelli, 1978), depending on cloud conditions, we assume that Eq. (10) holds nonetheless for all ice particle sizes for the sake of simplicity.

For reasons explained in section 3.3, our quantity of interest is not the number concentration, but rather the volume fraction ϕ of hydrometeors in clouds, which can be obtained by integrating the corresponding moment of the Marshall-Palmer distribution, i.e.

$$\phi = \int_0^\infty \frac{\pi D^3}{6} N_0 \exp(-\lambda D)\,\mathrm{d}D.$$

$$\phi = \int_0^\infty \frac{\pi D^3}{6} \bar{N}_{met}(D)\,\mathrm{d}D. \tag{13}$$

In order to determine the wake regimes from the size distribution, the terminal velocity needs to be approximated as a function of the ice particle diameter, and hence, further assumptions on the density of the ice particles have to be made. For graupel particles, the density may take values which range between $0.05\,\mathrm{g\,cm}^{-3}$ and $0.89\,\mathrm{g\,cm}^{-3}$, depending on growth conditions and history (Pruppacher and Klett, 2010). For our estimation we choose a value of $0.6\,\mathrm{g\,cm}^{-3}$, as we are primarily concerned with ice particles in the wet-growth mode, which typically constitute the upper end of the density range. Using this value and the empirical drag law of Schiller and Naumann (1933), the critical diameters for regime transition are calculated from the critical Reynolds numbers assuming a fluid density of $1\mathrm{kg\,m}^{-3}$ and a kinematic viscosity of $1.68 \cdot 10^{-5}\mathrm{m}^2\mathrm{s}^{-1}$, which corresponds approximately to the values expected at 750kPa air pressure and $-10°\mathrm{C}$ ambient temperature (see table 1). The total solid volume fraction can then be subdivided into the contributions by ice particles with a certain wake regime, i.e.

$$\phi \equiv \sum_j \phi_j = \sum_j \int_{D_{j,\min}}^{D_{j,\max}} \frac{\pi D^3}{6} N_0 \exp(-\lambda D)\,\mathrm{d}D,$$

$$\phi \equiv \sum_j \phi_j = \sum_j \int_{D_{j,\min}}^{D_{j,\max}} \frac{\pi D^3}{6} \bar{N}_{met}(D)\,\mathrm{d}D, \tag{14}$$

where the index j denotes one of the four wake regimes (steady axisymmetric; steady oblique; oscillating oblique; chaotic) and $D_{j,\min}$, $D_{j,\max}$ the corresponding lower/upper limit for the hydrometeor diameter to be in this regime.

regime	axisymmetric	steady oblique	oscillating oblique	chaotic
Re_c	212	273	360	–
$D_{j,\min}$	0	1.08 mm	1.24 mm	1.44 mm
$D_{j,\max}$	1.08 mm	1.24 mm	1.44 mm	∞

Table 1. Summary of the critical Reynolds numbers for regime transition and the threshold diameters used to determine the partial volume fractions.

Figure 2 shows the estimated volume fraction of frozen hydrometeors in clouds as a function of cloud temperature. The values are typically smaller than 10^{-5} and decrease exponentially with decreasing temperature. When comparing the various regimes, it can be observed that the largest contributions generally stem from hydrometeors in the axisymmetric or chaotic regime. This becomes especially clear when looking at the relative contribution of ϕ_j to the total volume fraction ϕ as shown in fig. 3. As can be seen, more than 80% of ice particles (by volume) exhibit one of these two wake regimes. Chaotic wakes are dominant at temperatures close to the freezing point, while axisymmetric wakes dominate when the temperature is very low. We will therefore focus solely on the axisymmetric and chaotic regimes in the following.

3.2 Supersaturation in the wake of hydrometeors

We now examine the saturation profiles in the wake of hydrometeors in the two regimes of interest. Figure 4 shows isocontours of supersaturation w.r.t. ice, defined as $s_i = S_i - 1$, for two different values of the Reynolds number, namely $Re = 75$, which lies within the axisymmetric regime, and $Re = 600$ in the chaotic wake regime. ~~As ambient temperature ,~~ The ambient temperature was set to a value of ~~$T_\infty = -30°C$ was adopted, because this roughly corresponds to the cloud temperature where the two regimes are of equal significance (cf. fig. 3).~~ $T_\infty = -15°C$, i.e. the temperature gap between the ambient air and the meteor surface is 15K, which corresponds to rather extreme cloud conditions with high liquid water contents (Greenan and List, 1995) . Since the ambient fluid is already supersaturated w.r.t. ice, the threshold of the isocontours is given as an excess to the value in the ambient~~and we define the excess supersaturation as~~

$\tilde{s} \equiv s - s_\infty.$

At $Re = 75$, the flow is steady, and thus, so is the supersaturation field. In the chaotic regime, the flow is characterized by time-dependent vortex shedding from the ice particle's boundary layer, and therefore excess supersaturation appears intermittently. In both regimes, significant excess supersaturation w.r.t. the ambient can be observed far downstream and the volume of air which is affected by the wake is by far larger than the volume of the meteor. This can be seen more clearly when averaging the fields in the azimuthal direction, which is statistically homogeneous for both cases, as well as in time for the unsteady flow. The averaged excess supersaturation w.r.t. ice is shown in fig. 5 for both cases. The saturation profiles differ substantially from the ones obtained by Fukuta and Lee (1986) for similar boundary conditions and Reynolds number. This is presumably due to their strong simplification of potential flow, which is incapable of reproducing the boundary layer and the flow in the wake of the ice particle correctly. This indeed leads to strong modifications in the distribution of supersaturated regions. Regions of high vapor content and relatively low temperatures, i.e. supersaturated regions, which are created in the mixing layer close to the riming particle are transported further downstream by the detaching vortices in the chaotic regime. This ~~effect~~ phenomenon does not occur in the simulations of Fukuta and Lee (1986), who observed a complete decay of supersaturation to the inflow value within ~~a distance of approximately $2.5D$ downstream of the ice particle for $T_\infty = -30°\mathrm{C}$~~ few meteor diameters downstream (approximately within two diameters at $-20°\mathrm{C}$), while fig. 5 clearly indicates that regions with ~~$\tilde{s}_i > 0$~~ $s_i(\boldsymbol{x},t) > s_{i,\infty}$ may be observed at ~~distances more than $50D$ from the rear at this temperature.~~ downstream distances of the order of $50D$ at $-15°\mathrm{C}$.

In order to compare the induced supersaturation for different values of T_∞ and in between different regimes, we compute the time-averaged volume of air which is supersaturated above a given threshold,

$$V_s(s^*) \equiv \frac{1}{\tau} \int_0^\tau \int_\Omega H(s(\boldsymbol{x},t) - s^*) \,\mathrm{d}\Omega \,\mathrm{d}t,$$

$$V_s(s^*) \equiv \int_\Omega \langle H(s(\boldsymbol{x},t) - s^*) \rangle_t \,\mathrm{d}\boldsymbol{x}, \tag{15}$$

where V_s is the superaturated volume, s^* the corresponding threshold and H the Heaviside step function. The integral is to be understood as a volume integral over the simulation domain Ω and $\langle . \rangle_t$ denotes the time-averaging operator. The supersaturated volume can be computed w.r.t. ice or the liquid phase which will be indicated in the following by a phase subscript for the threshold variable.

Figure 6 shows ~~this quantity normalized by the volume of the ice particle~~ the normalized volume of air superaturated w.r.t. ice (a) and liquid (b) as a function of the ~~threshold~~thresholds s_i^* and s_w^*, respectively. It can be seen ~~,~~ that in the axisymmetric regime, the supersaturated volume is generally larger than in the chaotic regime. This is caused by the enhanced mixing properties of the vortical wake structures in the latter case, which lead to a faster decay of the scalar field.

For both regimes, the range of observed values of supersaturation is similar. In fact, differences in range may only occur due to the distinct diffusivities of the temperature and water vapor fields, which indeed lead to subsaturations in the chaotic regime in some parts of the flow. While the range can be estimated reasonably well using simple mixing arguments (Chouippe

et al., 2019), we observe that the highest values of supersaturation only occur in a very confined portion of the wake. However, if the temperature difference between the ambient and the ice particle is sufficiently high, a strong excess in supersaturation compared to the ambient value may occur for both phases in a volume comparable to the size of the meteor, if no mechanism for depletion is considered. ~~This excess may be as high as 270% at a temperature difference of 40K. For all values of T_∞ the~~ The volume of air which is affected by the wake-induced supersaturation is of the order of 10^3 particle volumes for all temperature gaps of interest.

3.3 Ice enhancement due to meteor wakes

~~Our spatially resolved data allows us, for the first time to our knowledge, to quantify the significance of wake-induced supersaturation on ice enhancement. Thus, in this section, we are now aiming to estimate how the nucleation of ice~~ In the previous section it was shown that considerable supersaturations may be observed in the wake of hydrometeors and that the volume of air which is affected by ~~this excess in supersaturation. We therefore adopt the commonly used ice enhancement factor (e.g. Baker, 1991), which is defined as the ratio between the observed number concentration of~~ it is far larger than what has been previously estimated in the literature. In order to analyze our spatially resolved data in terms of ice nucleation, a constitutive relation is required which links supersaturation to the concentration of activated ice nuclei (IN)~~and that expected for a reference state. For our problem, it will be defined as~~

~~$$f_i \equiv \frac{N_{IN}\,\text{(with meteors)}}{N_{IN}\,\text{(without meteors)}}.$$~~

. A possible parametrization obtained from continuous-flow diffusion chamber (CFDC) measurements for natural aerosols is given by Meyers et al. (1992) and reads

$$N_{IN} = 0.528 \exp\left(12.96 s_i\right) \mathrm{m}^{-3}. \tag{16}$$

~~The IN number concentration~~ Here, N_{IN} ~~, i.e. those aerosol particles which can be activated at a given supersaturation, is commonly approximated by a power-law in terms of the supersaturation w.r.t. ice,~~

~~$$N_{IN} = C s_i^\alpha$$~~

~~where C, α are constants depending on the aerosol composition (Huffman, 1973). For natural aerosols, the exponent α typically ranges between 3 and 8, where larger values are attributed to more polluted air masses, e. g. near metropolitan or industrial areas (Pruppacher and Klett, 2010). We are aware that~~ denotes the number concentration of IN activated by the deposition and condensation-freezing mechanisms. Eq. ~~is a very simplified approach to the problem and its validility might be debatable. In particular, it does not take into account the various characteristics of~~ (16) is reported to be strictly valid in the parameter range

$$-20°\mathrm{C} < T < -7°\mathrm{C}, \quad 0.02 < s_i < 0.25, \quad -0.05 < s_w < 0.045, \tag{17}$$

which corresponds to the range of the underlying CFDC data, albeit it has also been applied outside of this range (Meyers et al., 1992) . The temperatures of interest in the current work fall well into the ~~different freezing modes, which are dependent on the~~

~~temperature and~~ range of validity. As the distribution of s_i in the wake (fig. 6a) shows, s_i does only slightly exceed 25% at the lowest ambient temperature considered. However, only a small portion of the wake exhibits such high values, and hence, imprecisions are likely to be insignificant for integral quantities. The volumetric distribution of s_w (fig. 6b) indicates that super-
295 saturation w.r.t. ~~the liquid phase, nor the time scales of freezing, which might play an significant role in the microphysical view. The results should therefore only be regared as a first crude estimation on the importance of wake-induced ice enhancement in clouds.~~liquid exceeds the CFDC data range in significant portions of the wake when $T_\infty \lesssim -10°\mathrm{C}$. Therefore, the constitutive relation may underestimate the contribution of the condensation-freezing mode, as this mode exhibits increased activity under these conditions, as has been demonstrated by Schaller and Fukuta (1979) for various substances. Having this in mind, we are
300 not aware of any parametrization of condensation-freezing nucleation for natural aerosols which can be directly applied under these conditions.

~~Using Eq.~~

One way to quantify the enhancement of nucleation activity is the ice enhancement factor, i.e. the ratio between the observed number concentration of ice nuclei and that expected for a reference state. This concept has been used before by Baker (1991)
305 to study meteor-induced ice enhancement. For our problem, the local ice enhancement factor can be expressed as

$$f_i(\boldsymbol{x}) = \frac{\langle s_i^\alpha \rangle_t(\boldsymbol{x})}{s_{i,\infty}^\alpha}.$$

$$f_i(\boldsymbol{x}) = \frac{\langle N_{IN}(\boldsymbol{x},t)\rangle_t}{N_{IN,\infty}}, \tag{18}$$

~~This quantity~~ where $N_{IN}(\boldsymbol{x},t)$ is calculated from the instantaneous local supersaturation w.r.t. ice using Eq. (16) and $N_{IN,\infty}$
310 is the IN concentration evaluated for ambient conditions. Thus, the ice enhancement factor gives a quantitative measure on how ~~much more ice is produced~~ many additional IN are activated in the wake of the hydrometeor compared to the ambient~~under the limitations stated above. Figure ?? shows how the ice enhancement is distributed~~.

Figure 7 visualizes the local ice enhancement factor in the wake of a hydrometeor at ~~$T_\infty = -30°\mathrm{C}$ for an exponent of $\alpha = 8$~~$T_\infty = -15°\mathrm{C}$. At this rather favorable parameter point, ~~which can be considered as rather favorable,~~ we observe that ~~f_i~~
315 ~~can locally reach extremely high values of the order of 10^4~~ ice nucleation is considerably increased (up to a factor of 6) in the near vicinity of the hydrometeor and significant values ~~greater than 10 can~~ may still be observed in the far wake. It is therefore conceivable that a considerable amount of new ice may be formed in the wake, which is consistent with recent experimental results of Prabhakaran et al. (2020) who observed nucleation of water droplets and ice particles in the wake of a hot drop under cold conditions.

320 Using Eq. (16), the supersaturated volume can be expressed as a function of the ice enhancement factor in order to gain insight into the volumetric distribution of f_i. Figure 8 shows the distributions for ~~$\alpha = 8$ and~~ various temperatures in both wake regimes. The ice enhancement is generally higher in the axisymmetric regime than in the chaotic regime. Please note, that for a more precise analysis of this behavior, the actual flow-driven distribution of ~~aerosol particles~~ AP in the wake should be

considered. Depending on the flow dynamics, ice nucleating particles ~~might~~ may accumulate in the wake or be expelled from it (Homann and Bec, 2015), which might have a non-negligible impact on ice enhancement. However, the consideration of aerosol dynamics is outside the scope of the present work.

~~We therefore conclude~~ The analysis of the local ice enhancement factor leads to the conclusion that the wake of a hydrometeor may act as a site of increased nucleation activity, and that the volume in which this increased activity occurs is much larger than the volume of the hydrometeor itself. ~~This conclusion is consistent with recent experimental results of Prabhakaran et al. (2019) who observed nucleation of water droplets and ice particles in the wake of a hot drop under cold conditions with a temperature difference comparable to the one presented in fig. **??**.~~

Having identified wake-induced supersaturation as a possible ice multiplication mechanism in the near surrounding of a hydrometeor, its significance in the larger context of clouds is yet to be investigated. In order to assess ~~the significance of the wake effect in clouds, a global~~ this, we suggest to compute a coarse-grained ice enhancement factor~~needs to be computed~~, which takes into account the spatial distribution of f_i obtained by the numerical simulations, as well as the ~~volumetric ice concentration . We~~ concentration of primary ice particles. Therefore, we define a control volume $\mathcal{V}$ within a cloud which is sufficiently large such that the hydrometeor size distribution follows Eq. (10), but sufficiently small such that the saturation field is uniform (with a value of $s_{i,\infty}$) if no hydrometeor is present. The volume-averaged ice enhancement factor within this control volume is given by

$$\langle f_i \rangle_{\mathcal{V}} = \frac{\int_{\mathcal{V}} (f_i(\boldsymbol{x}) - 1)\,\mathrm{d}\mathcal{V}}{\int_{\mathcal{V}} \mathrm{d}\mathcal{V}} + 1,$$

$$\langle f_i \rangle_{\mathcal{V}} = \frac{\int_{\mathcal{V}} (\langle N_{IN}(\boldsymbol{x},t)\rangle_t - N_{IN,\infty})\,\mathrm{d}\boldsymbol{x}}{\int_{\mathcal{V}} N_{IN,\infty}\,\mathrm{d}\boldsymbol{x}} + 1, \tag{19}$$

where the integral has been decomposed into an excess contribution, which evaluates to zero outside of the wake, and a base contribution, which is equal to unity. At sufficiently small volume fractions, the wakes of individual hydrometeors can be assumed to not interact, and hence, the integral in the enumerator of the first term in Eq. (19) can be expressed as a sum of contributions from independent hydrometeors, i.e.

$$\int_{\mathcal{V}} (f_i(\boldsymbol{x}) - 1)\,\mathrm{d}\mathcal{V} = \sum_{(k)} \int_{\Omega^{(k)}} (f_i(\boldsymbol{x}) - 1)\,\mathrm{d}\Omega^{(k)},$$

$$\int_{\mathcal{V}} (\langle N_{IN}(\boldsymbol{x},t)\rangle_t - N_{IN,\infty})\,\mathrm{d}\boldsymbol{x} = \sum_{(k)} \int_{\Omega^{(k)}} (\langle N_{IN}(\boldsymbol{x},t)\rangle_t - N_{IN,\infty})\,\mathrm{d}\boldsymbol{x}, \tag{20}$$

where $\Omega^{(k)} \subseteq \mathcal{V}$ ~~denotes the simulation domain scaled by the size of particle~~ indicates that the field $N_{IN}(\boldsymbol{x},t)$ is to be taken from a simulation with an appropriate value of the Reynolds number for meteor (k). ~~By defining the excess ice enhancement~~

~~per meteor volume as~~

$$\tilde{f}_{i,\Omega^{(k)}} \equiv \frac{6}{\pi D^3} \int_{\Omega^{(k)}} (f_i(\boldsymbol{x}) - 1)\, \mathrm{d}\Omega^{(k)}$$

~~and assuming~~ . Assuming a continuous particle size distribution ~~following~~ according to Eq. (10), the volume-averaged ice enhancement within $\mathcal{V}$ can be expressed as

$$\langle f_i \rangle_{\mathcal{V}} = 1 + \int_0^\infty \tilde{f}_{i,\Omega} \frac{\pi D^3}{6} N_0 \exp(-\lambda D)\, \mathrm{d}D.$$

$$\langle f_i \rangle_{\mathcal{V}} = 1 + \frac{1}{N_{IN,\infty}} \int_0^\infty \bar{N}_{met}(D) \int_{\Omega(D)} (\langle N_{IN}(\boldsymbol{x},t) \rangle_t - N_{IN,\infty})\, \mathrm{d}\boldsymbol{x}\, \mathrm{d}D, \tag{21}$$

~~Since $\tilde{f}_{i,\Omega}$ is normalized by the volume of the ice particle, its value only depends on the flow field in~~ where $\Omega(D)$ denotes the simulation domain for a meteor with diameter D. An evaluation of this expression requires knowledge on how the supersaturation field evolves with the Reynolds number. However, our results for the two regimes investigated indicate that the values of the non-dimensional ~~form, i. e. the diameter dependency only enters through the value of the Reynolds number~~integral

$$\tilde{I}_{\Omega(D)} \equiv \frac{6}{\pi} \int_{\Omega(D)} (\langle N_{IN}(\tilde{\boldsymbol{x}},t) \rangle_t - N_{IN,\infty})\, \mathrm{d}\tilde{\boldsymbol{x}} \tag{22}$$

is of the same order of magnitude for a wide range of Reynolds number, as they only differ approximately by a factor of 3 for the two Reynolds numbers investigated. For reasons of simplicity, we ~~assume that $\tilde{f}_{i,\Omega}$~~ therefore assume that $\tilde{I}_{\Omega(D)}$ can be approximated for a given regime by the value determined for a single Reynolds number within that regime, $\tilde{I}_{\Omega_j}$, which allows us to rewrite Eq. (21) in the simplified form

$$\langle f_i \rangle_{\mathcal{V}} = 1 + \sum_j \phi_j \tilde{f}_{i,\Omega_j},$$

$$\langle f_i \rangle_{\mathcal{V}} = 1 + \frac{1}{N_{IN,\infty}} \sum_j \int_{D_{j,\min}}^{D_{j,\max}} \frac{\pi D^3}{6} \bar{N}_{met}(D) \tilde{I}_{\Omega_j}\, \mathrm{d}D. \tag{23}$$

~~where ϕ_j is the volume fraction of meteors in regime j, as defined in~~ Since $\tilde{I}_{\Omega_j}$ is now a constant for each regime, this can be reexpressed using Eq. (14) ~~, and $\tilde{f}_{i,\Omega_j}$ the value of the excess ice enhancement evaluated for a single value of the Reynolds~~

~~number in that regime~~to yield

$$\langle f_i \rangle_{\mathcal{V}} = 1 + \sum_j \phi_j \tilde{I}_{\Omega_j} / N_{IN,\infty}, \tag{24}$$

which demonstrates the importance of the ice volume fraction on global ice enhancement. As has already been discussed and shown in fig. 3, the axisymmetric and chaotic regimes contribute the most to the volume fraction. We therefore disregard the contribution of the two other regimes and adjust the threshold of regime transition accordingly ~~.~~

~~$\langle f_i \rangle_{\mathcal{V}} = 1 + \phi_{axi} \tilde{f}_{i,\Omega_{axi}} + \phi_{cha} \tilde{f}_{i,\Omega_{cha}}$~~

to a value of $1.26\,\mathrm{mm}$, which allows us to evaluate Eq. (24) from our flow simulation data.

Both ϕ_j and ~~$\tilde{f}_{i,\Omega}$~~ $\tilde{I}_{\Omega_j}$ are functions of ambient temperature, and thus the global ice enhancement factor originating from meteor wakes can be expressed as a function of cloud temperature. While the former decreases exponentially with decreasing temperature, the latter exhibits a strong increase leading to a counteracting effect. Furthermore, a large number of ice particles pertain to the axisymmetric regime for low temperatures, which is slightly more favorable in terms of ice enhancement.

Please be aware that, even though our aim is to quantify the wake-induced ice formation, the volume fraction of ice will be regarded as constant. The reason for this is that the approach used in this study does not allow us to derive the time scales of ~~nucleation nor growth of~~ growth for newly created ice, and thus, the time-dependent coupling with the size distribution is inaccessible. Therefore, the following considerations merely apply to the initial state of a possible rapid glaciation process.

Figure 9 shows the global ice enhancement factor as a function of ambient temperature~~for different values of α, the exponent in Eq.~~. It can be seen that ~~significant ice enhancement in the global sense only occurs at cloud temperatures below $-30\,^{\circ}\mathrm{C}$ in conjunction with high values of α. Even then, the enhancement is only marginal with $\langle f_i \rangle_{\mathcal{V}}$ being smaller than 8. We therefore~~ ice nucleation in a given cloud volume is only marginally increased due to the presence of meteor wakes. At the highest temperature gap considered, the induced supersaturation activates roughly 0.08% more ice than the ambient, and hence, we conclude that under typical cloud conditions ~~hydrometeors do not directly lead to substantially enhanced~~ hydrometeor wakes do not considerably affect ice nucleation on a ~~global scale~~cloud scale, at least when the volume fraction of ice in the cloud is as low as predicted by the parametrization of Houze et al. (1979).

~~Since the small volume fraction of ice~~ Since the volume fraction is the limiting factor for ice enhancement~~on a global scale~~, we revisited our assumption on the size distribution of ice particles in order to assess the sensitivity to the parametrization. Using the parametrization of Heymsfield et al. (2002) for deep subtropical and tropical clouds, the ice volume fraction ~~may be up to five times larger at $T_\infty = -40\,^{\circ}\mathrm{C}$. However,~~ is of the same order of magnitude as for the presented results, such that the conclusions which have been drawn for frontal clouds also persist for this type of cloud.

3.4 Time scales of nucleation and history effects

The ice enhancement analysis presented in the previous subsection did not explicitly address two factors which may be of importance when investigating IN activation, namely the time of exposure required to actually activate an AP and history

effects, i.e. the circumstance that IN which have been activated in the wake may stay activated once they are not exposed to the wake anymore. The latter leads to an accumulative effect, which suggests that it is more reasonable to consider the volume swept by the meteors rather then looking at the volume within a cloud which is instantaneously exposed to high supersaturations. Indeed, Prabhakaran et al. (2020) used this argument to show that essentially all interstitial AP within a cloud volume of interest are exposed to high supersaturations within a few minutes. Following their arguments, we estimated the time required to expose a significant portion of the cloud to the wakes using

$$\tau_{sweep} = \left(\int_0^\infty \bar{N}_{met}(D) \dot{V}_{sweep}(D) \, \mathrm{d}D \right)^{-1}, \tag{25}$$

where $\dot{V}_{sweep} = \epsilon v_p D^2 \pi / 4$ is the volumetric flow rate of air which is swept by a hydrometeor with diameter D and velocity v_p and ϵ being an unknown factor assumed to be of the order of unity. Using the size distribution of Houze et al. (1979) and the terminal velocity for smooth spheres, we obtain $\tau_{sweep} \approx 110\mathrm{s}$ at ~~higher cloud temperatures, i. e. when the temperature difference between ice particles and the ambient is moderate, the volume fraction is of the same order of magnitude as for the presented results, such that the conclusions which have been drawn for frontal clouds also persist for this type of cloud.~~ $-15°\mathrm{C}$, which fits the estimation of Prabhakaran et al. (2020) very well. The use of an empirical law for the terminal velocity of frozen hydrometeors of natural shape leads to larger values of τ_{sweep}, which are, however, found to be of similar order of magnitude.

In the following we apply the swept-volume argument to ice multiplication by quantifying the excess ice nucleation rate induced by the meteor wakes, henceforth denoted as j_{met}. Under the assumption that nucleation occurs sufficiently fast to achieve the IN concentrations predicted by Eq. (16), the nucleation rate can be estimated from the number of IN activated in the wake and the time it takes to replenish the volume of fluid affected by high supersaturations. The former is obtained directly from our simulation data by computing the volume integral $\int_{\Omega(D)} (\langle N_{IN}(\boldsymbol{x},t) \rangle_t - N_{IN,\infty}) \, \mathrm{d}\boldsymbol{x}$ while the latter is difficult to define objectively. We propose to estimate the time scale of wake renewal by

$$\tau_{expo} \equiv V_{aff} / \dot{V}_{sweep} \tag{26}$$

where $V_{aff} = \gamma D^3 \pi / 6$ is the volume affected by the wake of a hydrometeor of diameter D, which should be proportional to the volume of the hydrometeor. The prefactor γ is currently unknown, but might be related to the concept of supersaturated volume. The time scale τ_{expo} can be interpreted as the characteristic time a fluid volume is exposed to high supersaturations, and hence the subscript. From the definitions of V_{aff} and $\dot{V}_{sweep}$ it follows that $\tau_{expo} \propto D / v_p$ with the constant of proportionality being referred to as C_{expo} hereafter. This new constant contains both unknown coefficients ϵ and γ and might be understood as the non-dimensional streamwise length of the wake. Again, this length is difficult to define rigorously due to the asymptotic decay of supersaturation, but judging from fig. 7, it is likely of the order of 10. The swept-volume limited nucleation rate for

an ensemble of meteors is then given by

$$j_{met}^{expo} = \int_0^\infty \bar{N}_{met}(D) \frac{1}{\tau_{expo}(D)} \int_{\Omega(D)} \left(\langle N_{IN}(\boldsymbol{x},t) \rangle_t - N_{IN,\infty} \right) \mathrm{d}\boldsymbol{x}\, \mathrm{d}D \tag{27}$$

under the assumptions that IN activate sufficiently fast during the exposure, a sufficient number of activatable AP is present and that those are homogeneously distributed within the wake. The resulting nucleation rate is displayed in fig. 10 for $C_{expo} = 10$ (solid blue line) and the range $1 < C_{expo} < 100$ in order to pay regard to the uncertainties associated with this tunable parameter (shaded blue area). Under the assumptions just stated, meteor-wakes indeed appear to be capable of activating a large number of IN in a short amount of time, as has been concluded by Prabhakaran et al. (2020). In fact, at $-10°\mathrm{C}$ it would only take around 40s for the number concentration of wake-activated IN to match the concentration of primary meteors.

This result strongly contradicts our conclusion that wake-induced supersaturation is of little significance in clouds based on the ice enhancement factor. As will be demonstrated in the following, the resolution to this apparent contradiction requires an examination of the time scales of nucleation and exposure. For $C_{expo} = 10$, the exposure times are of the order of 5ms for all diameters of interest, which is substantially shorter than the time scales usually relevant for cloud modelling (of the order of minutes). As Eq. (16) has been developed for cloud modelling, the validity of the assumption that IN activation can be regarded as instantaneous at the time scales considered should be brought into question. Indeed, classical nucleation theory (Fletcher, 1958) suggests that nucleation is a time-dependent process until the activated fraction of AP approaches unity. From concentrations of IN obtained from continuous-flow diffusion chamber (CFDC) experiments, the nucleation rate may be estimated by taking into account the residence time in the apparatus, τ_{nucl} (Hoose and Möhler, 2012). Since Eq. (16) is based on CFDC data, we make the conjecture that the local nucleation rate may be approximated by the relationship

$$j_{IN}(\boldsymbol{x},t) \approx N_{IN}(\boldsymbol{x},t)/\tau_{nucl}. \tag{28}$$

In Hoose and Möhler (2012) residence times ranging from 1.6s to 120s are reported for various CFDC experiments. The primary data used to obtain Eq. (16) also suggests that the peak concentration N_{IN} is achieved with residence times of approximately 10s (Al-Naimi and Saunders, 1985) and that shorter residence times lead to lower concentrations, which is in accordance to the arguments stated above. The crucial assumption of Eq. (27) that IN concentrations predicted by Eq. (16) can be achieved within the exposure time is disproved by acknowledging that $\tau_{nucl} \gg \tau_{expo}$. The large discrepancy in time scales suggests that the nucleation rate is not limited by the rate at which interstitial AP are entrained into the wake (the swept volume), but rather by the time scale of the nucleation process itself, and thus by the instantaneously exposed volume. A more appropriate estimate of the nucleation rate is then given by

$$j_{met}^{nucl} = \int_0^\infty \bar{N}_{met}(D) \frac{1}{\tau_{nucl}} \int_{\Omega(D)} \left(\langle N_{IN}(\boldsymbol{x},t) \rangle_t - N_{IN,\infty} \right) \mathrm{d}\boldsymbol{x}\, \mathrm{d}D \tag{29}$$

under the assumption that AP are entrained sufficiently fast into the wake, which seems reasonable given the arguments by Prabhakaran et al. (2020), and that they are distributed homogeneously within the wake. The new estimation of the nucleation

rate is shown in fig. 10 for $\tau_{nucl} = 10\text{s}$ (solid red line) and the range $1\text{s} < \tau_{nucl} < 100\text{s}$ (shaded red area). As can be seen, the rates are several orders of magnitude smaller than what has been previously estimated, and it would now take around 82h for the number concentration of wake-activated IN to match the concentration of primary meteors, which is in better agreement to the conclusion obtained with the help of the ice enhancement factor. In fact, it is straightforward to demonstrate that these two quantities are directly linked by the relationship

$$\langle f_i \rangle_{\mathcal{V}} = \frac{j_{met}^{nucl}}{N_{IN,\infty}/\tau_{nucl}} + 1. \tag{30}$$

Furthermore, it can be shown that as soon as a significant cloud volume is swept quickly at low volume fractions, the exposure time will automatically be short as $\tau_{expo} \propto \tau_{sweep}$ for a given meteor concentration, and thus, ice enhancement is again found to be limited by the low volumetric concentration of ice in clouds.

4 Conclusion

In this study we have performed numerical simulations of momentum, heat and mass transfer around a warm hydrometeor in order to assess the distribution of supersaturation in its wake, and moreover, the implications on ice nucleation enhancement. Our simulation method is based on a body-conforming spectral/spectral-element discretization and all relevant scales of the flow problem have been resolved. The hydrometeor is assumed to be of spherical shape and to possess a uniform surface temperature of 0 °C, while the ambient temperature has been varied in a range between ~~−40 °C~~ −15 °C and 0 °C. The vapor concentration is kept at saturation value with respect to ice at the particle surface, while it is saturated with respect to water in the ambient (reflecting the presence of supercooled droplets). Two different values of the Reynolds number have been simulated in order to capture the characteristics of the most relevant wake regimes, namely $Re = 75$, where the wake is steady and axisymmetric, and $Re = 600$, where the wake is chaotic.

We found that significant values of supersaturation can be attained in the wake of warm hydrometeors, which persist long enough to be observed at ~~more than 50~~ several tens of particle diameters downstream of the meteor for sufficiently high differences in temperature. The supersaturated volume of air exceeds the estimations by Fukuta and Lee (1986) by far, which is attributed to the more accurate representation of the flow in the current study. This is an important observation since one of the key arguments for disregarding wake-induced ice nucleation is the proclaimed small zone of influence (Baker, 1991). It should be borne in mind that the ambient air was considered to be quiescent in this study. Under atmospheric conditions, turbulent fluctuations with scales comparable in size with the hydrometeors are expected to be present, which will presumably lead to a faster decay of the vapor concentration and temperature in the wake (Bagchi and Kottam, 2008). It could be worthwhile to investigate the influence of turbulence on the supersaturated volume in the future, as well as the importance of fluctuations in the ambient saturation ratios in comparison to wake-induced fluctuations.

Using a ~~power-law approximation~~ constitutive relation provided by Meyers et al. (1992) for the ice ~~enhancement factor, we estimate~~ nuclei concentration, we estimated that heterogeneous nucleation may be locally enhanced by a factor ~~comparable to the discrepancy between ice nuclei and ice particles observed in field measurements~~of up to 6 if the temperature gap between the

ambient and the meteor's surface is sufficiently large. This enhancement increases strongly with decreasing cloud temperature and so does the affected volume of air, which is typically of the order of several hundred particle ~~diameters. However,~~ volumes. It is therefore conceivable that ice multiplication can be triggered by the meteor's wakes, which is in agreement with the recent experimental observations by Prabhakaran et al. (2020). However, as arguments on upscaling have shown, this local effect alone presumably has little significance in clouds due to the low volumetric concentration of ~~ice in clouds, this local effect alone unlikely serves as an explanation for the global discrepancy, as arguments on upscaling have shown .~~ primary ice. This conclusion appears contradictory to the arguments given by Prabhakaran et al. (2020), who assessed that hydrometeors are capable of sampling a large cloud volume with their wakes within a short amount of time. While this is indeed the case, we have shown that the time during which ice nucleating particles are exposed to the wake is generally too short to activate all of them, even at high values of supersaturation. The nucleation rate is therefore not limited by the rate at which interstitial AP are encountered, and therefore, the instantaneously exposed volume is argued to be more relevant, supporting the results obtained with the help of the ice enhancement factor.

In order for wake-induced supersaturation to be a relevant SIP, the nucleation rate needs to be considerably higher than what has been estimated in this work. While it might be possible that the condensation-freezing mode has been underestimated in this work, it seems unlikely that this underestimation is significant enough to substantially affect the conclusion. As the relevance of this SIP is mainly determined by the volumetric concentration of ice particles, high contents of ice are necessary for it to be active. Furthermore, in order to achieve an adequate temperature difference between the ambient and the ice, high liquid water contents are also required. Hence, if this SIP occurs in natural clouds, convective clouds are the most likely candidates.

Nonetheless, it is conceivable that the present mechanism in conjunction with one (or several) secondary ice processes is of greater relevance to the problem of ice formation. After a rapid glaciation process has been triggered, wake-induced nucleation might become significant, as the ice concentration then increases to considerable values. Futhermore, the question of whether or not wake-induced nucleation alone might trigger such a process has not been fully resolved yet, since the feedback on the size distribution of ice particles has been disregarded in this study. In order to assess this dynamical behavior, further time-resolved information on the ~~(pre-)~~activation of ice nuclei in the wake ~~currently~~ appears to be necessary. ~~This requires microphysical modeling of~~ By tracking the trajectories of AP, the estimation of the ~~nucleation process and knowledge on the spatial distribution of aerosol particles downstream of the ice particle. A~~ nucleation rate may be further improved and a resulting parametrization may be added to existing cloud models with explicit microphysics in order to assess the ~~evolution of the size distribution, and moreover, the relative significance~~ relative importance of wake-induced nucleation in comparison to other secondary ice processes.

Data availability. The datasets are available upon request to the corresponding author.

Author contributions. TL and MU conceptualized the idea. JD provided the simulation code and mesh. MK conducted the simulations. MK, AC and MU post-processed the data and TL assisted in the interpretation of the results. MK prepared and revised the manuscript and AC contributed to it. MU, AC, JD and TL proofread the manuscript.

Competing interests. The authors declare that they have no conflict of interest.

Acknowledgements. The authors thank Alexei Kiselev for ~~useful discussions~~helpful discussions. The constructive feedback by Alexei Korolev and an anonymous reviewer is greatly acknowledged as their suggestions helped to improve and clarify this manuscript. The simulations were partially performed at the Steinbuch Centre for Computing in Karlsruhe and the computer resources, technical expertise and assistance provided by this center are thankfully acknowledged.

References

Al-Naimi, R. and Saunders, C. P. R.: Measurements of Natural Deposition and Condensation-Freezing Ice Nuclei with a Continuous Flow Chamber, Atmospheric Environment (1967), 19, 1871–1882, https://doi.org/10.1016/0004-6981(85)90012-5, 1985.

Auer, A. H., Veal, D. L., and Marwitz, J. D.: Observations of Ice Crystal and Ice Nuclei Concentrations in Stable Cap Clouds, Journal of the Atmospheric Sciences, 26, 1342–1343, https://doi.org/10.1175/1520-0469(1969)026<1342:OOICAI>2.0.CO;2, 1969.

Bacon, N. J., Swanson, B. D., Baker, M. B., and Davis, E. J.: Breakup of Levitated Frost Particles, Journal of Geophysical Research: Atmospheres, 103, 13 763–13 775, https://doi.org/10.1029/98JD01162, 1998.

Bagchi, P. and Kottam, K.: Effect of Freestream Isotropic Turbulence on Heat Transfer from a Sphere, Physics of Fluids, 20, 073 305, https://doi.org/10.1063/1.2963138, 2008.

Bagchi, P., Ha, M. Y., and Balachandar, S.: Direct Numerical Simulation of Flow and Heat Transfer From a Sphere in a Uniform Cross-Flow, Journal of Fluids Engineering, 123, 347–358, https://doi.org/10.1115/1.1358844, 2001.

Baker, B. A.: On the Nucleation of Ice in Highly Supersaturated Regions of Clouds, Journal of the Atmospheric Sciences, 48, 1904–1907, https://doi.org/10.1175/1520-0469(1991)048<1905:OTNOII>2.0.CO;2, 1991.

Bouchet, G., Mebarek, M., and Dušek, J.: Hydrodynamic Forces Acting on a Rigid Fixed Sphere in Early Transitional Regimes, European Journal of Mechanics - B/Fluids, 25, 321–336, https://doi.org/10.1016/j.euromechflu.2005.10.001, 2006.

Chouippe, A., Krayer, M., Uhlmann, M., Dušek, J., Kiselev, A., and Leisner, T.: Heat and Water Vapor Transfer in the Wake of a Falling Ice Sphere and Its Implication for Secondary Ice Formation in Clouds, New Journal of Physics, 21, 043 043, https://doi.org/10.1088/1367-2630/ab0a94, 2019.

de Stadler, M. B., Rapaka, N. R., and Sarkar, S.: Large Eddy Simulation of the near to Intermediate Wake of a Heated Sphere at Re=10,000, International Journal of Heat and Fluid Flow, 49, 2–10, https://doi.org/10.1016/j.ijheatfluidflow.2014.05.013, 2014.

Dye, J. E. and Hobbs, P. V.: The Influence of Environmental Parameters on the Freezing and Fragmentation of Suspended Water Drops, Journal of the Atmospheric Sciences, 25, 82–96, https://doi.org/10.1175/1520-0469(1968)025<0082:TIOEPO>2.0.CO;2, 1968.

Field, P. R., Lawson, R. P., Brown, P. R. A., Lloyd, G., Westbrook, C., Moisseev, D., Miltenberger, A., Nenes, A., Blyth, A., Choularton, T., Connolly, P., Buehl, J., Crosier, J., Cui, Z., Dearden, C., DeMott, P., Flossmann, A., Heymsfield, A., Huang, Y., Kalesse, H., Kanji, Z. A., Korolev, A., Kirchgaessner, A., Lasher-Trapp, S., Leisner, T., McFarquhar, G., Phillips, V., Stith, J., and Sullivan, S.: Secondary Ice Production: Current State of the Science and Recommendations for the Future, Meteorological Monographs, 58, 7.1–7.20, https://doi.org/10.1175/AMSMONOGRAPHS-D-16-0014.1, 2017.

Fletcher, N. H.: Size Effect in Heterogeneous Nucleation, The Journal of Chemical Physics, 29, 572–576, https://doi.org/10.1063/1.1744540, 1958.

Fukuta, N. and Lee, H. J.: A Numerical Study of the Supersaturation Field around Growing Graupel, Journal of the Atmospheric Sciences, 43, 1833–1843, https://doi.org/10.1175/1520-0469(1986)043<1833:ANSOTS>2.0.CO;2, 1986.

Gagin, A.: The Effect of Supersaturation on the Ice Crystal Production by Natural Aerosols, Journal de Recherches Atmosphériques, 6, 175–185, 1972.

Ghidersa, B. and Dušek, J.: Breaking of Axisymmetry and Onset of Unsteadiness in the Wake of a Sphere, Journal of Fluid Mechanics, 423, 33–69, https://doi.org/10.1017/S0022112000001701, 2000.

Gordon, G. L. and Marwitz, J. D.: An Airborne Comparison of Three PMS Probes, Journal of Atmospheric and Oceanic Technology, 1, 22–27, https://doi.org/10.1175/1520-0426(1984)001<0022:AACOTP>2.0.CO;2, 1984.

Greenan, B. J. W. and List, R.: Experimental Closure of the Heat and Mass Transfer Theory of Spheroidal Hailstones, Journal of the Atmospheric Sciences, 52, 3797–3815, https://doi.org/10.1175/1520-0469(1995)052<3797:ECOTHA>2.0.CO;2, 1995.

Hallett, J. and Mossop, S. C.: Production of Secondary Ice Particles during the Riming Process, Nature, 249, 26–28, https://doi.org/10.1038/249026a0, 1974.

Herzegh, P. H. and Hobbs, P. V.: Size Spectra of Ice Particles in Frontal Clouds: Correlations between Spectrum Shape and Cloud Conditions, Quarterly Journal of the Royal Meteorological Society, 111, 463–477, https://doi.org/10.1002/qj.49711146810, 1985.

Heymsfield, A. J., Bansemer, A., Field, P. R., Durden, S. L., Stith, J. L., Dye, J. E., Hall, W., and Grainger, C. A.: Observations and Parameterizations of Particle Size Distributions in Deep Tropical Cirrus and Stratiform Precipitating Clouds: Results from In Situ Observations in TRMM Field Campaigns, Journal of the Atmospheric Sciences, 59, 3457–3491, https://doi.org/10.1175/1520-0469(2002)059<3457:OAPOPS>2.0.CO;2, 2002.

Hobbs, P. V.: Ice Multiplication in Clouds, Journal of the Atmospheric Sciences, 26, 315–318, https://doi.org/10.1175/1520-0469(1969)026<0315:IMIC>2.0.CO;2, 1969.

Hobbs, P. V. and Alkezweeny, A. J.: The Fragmentation of Freezing Water Droplets in Free Fall, Journal of the Atmospheric Sciences, 25, 881–888, https://doi.org/10.1175/1520-0469(1968)025<0881:TFOFWD>2.0.CO;2, 1968.

Hobbs, P. V. and Rangno, A. L.: Ice Particle Concentrations in Clouds, Journal of the Atmospheric Sciences, 42, 2523–2549, https://doi.org/10.1175/1520-0469(1985)042<2523:IPCIC>2.0.CO;2, 1985.

Hogan, R. J., Field, P. R., Illingworth, A. J., Cotton, R. J., and Choularton, T. W.: Properties of Embedded Convection in Warm-Frontal Mixed-Phase Cloud from Aircraft and Polarimetric Radar, Quarterly Journal of the Royal Meteorological Society, 128, 451–476, https://doi.org/10.1256/003590002321042054, 2002.

Homann, H. and Bec, J.: Concentrations of Inertial Particles in the Turbulent Wake of an Immobile Sphere, Physics of Fluids, 27, 053 301, https://doi.org/10.1063/1.4919723, 2015.

Hoose, C. and Möhler, O.: Heterogeneous Ice Nucleation on Atmospheric Aerosols: A Review of Results from Laboratory Experiments, Atmospheric Chemistry and Physics, 12, 9817–9854, https://doi.org/10.5194/acp-12-9817-2012, 2012.

Houze, R. A., Hobbs, P. V., Herzegh, P. H., and Parsons, D. B.: Size Distributions of Precipitation Particles in Frontal Clouds, Journal of the Atmospheric Sciences, 36, 156–162, https://doi.org/10.1175/1520-0469(1979)036<0156:SDOPPI>2.0.CO;2, 1979.

Huffman, P. J.: Supersaturation Spectra of AgI and Natural Ice Nuclei, Journal of Applied Meteorology (1962-1982), 12, 1080–1082, 1973.

Jenny, M. and Dušek, J.: Efficient Numerical Method for the Direct Numerical Simulation of the Flow Past a Single Light Moving Spherical Body in Transitional Regimes, Journal of Computational Physics, 194, 215–232, https://doi.org/10.1016/j.jcp.2003.09.004, 2004.

Jenny, M., Dušek, J., and Bouchet, G.: Instabilities and Transition of a Sphere Falling or Ascending Freely in a Newtonian Fluid, Journal of Fluid Mechanics, 508, 201–239, https://doi.org/10.1017/S0022112004009164, 2004.

Johnson, T. A. and Patel, V. C.: Flow Past a Sphere up to a Reynolds Number of 300, Journal of Fluid Mechanics, 378, 19–70, https://doi.org/10.1017/S0022112098003206, 1999.

Koenig, L. R.: The Glaciating Behavior of Small Cumulonimbus Clouds, Journal of the Atmospheric Sciences, 20, 29–47, https://doi.org/10.1175/1520-0469(1963)020<0029:TGBOSC>2.0.CO;2, 1963.

Korolev, A., Heckman, I., Wolde, M., Ackerman, A. S., Fridlind, A. M., Ladino, L. A., Lawson, R. P., Milbrandt, J., and Williams, E.: A New Look at the Environmental Conditions Favorable to Secondary Ice Production, Atmospheric Chemistry and Physics, 20, 1391–1429, https://doi.org/10.5194/acp-20-1391-2020, 2020.

Kotouč, M., Bouchet, G., and Dušek, J.: Loss of Axisymmetry in the Mixed Convection, Assisting Flow Past a Heated Sphere, International Journal of Heat and Mass Transfer, 51, 2686–2700, https://doi.org/10.1016/j.ijheatmasstransfer.2007.10.005, 2008.

Kotouč, M., Bouchet, G., and Dušek, J.: Transition to Turbulence in the Wake of a Fixed Sphere in Mixed Convection, Journal of Fluid Mechanics, 625, 205, https://doi.org/10.1017/S0022112008005557, 2009.

Marshall, J. S. and Palmer, W. M. K.: The Distribution of Raindrops with Size, Journal of Meteorology, 5, 165–166, https://doi.org/10.1175/1520-0469(1948)005<0165:TDORWS>2.0.CO;2, 1948.

Meyers, M. P., DeMott, P. J., and Cotton, W. R.: New Primary Ice-Nucleation Parameterizations in an Explicit Cloud Model, Journal of Applied Meteorology, 31, 708–721, https://doi.org/10.1175/1520-0450(1992)031<0708:NPINPI>2.0.CO;2, 1992.

Mossop, S. C.: The Origin and Concentration of Ice Crystals in Clouds, Bulletin of the American Meteorological Society, 66, 264–273, https://doi.org/10.1175/1520-0477(1985)066<0264:TOACOI>2.0.CO;2, 1985.

Murphy, D. M. and Koop, T.: Review of the Vapour Pressures of Ice and Supercooled Water for Atmospheric Applications, Quarterly Journal of the Royal Meteorological Society, 131, 1539–1565, https://doi.org/10.1256/qj.04.94, 2005.

Nix, N. and Fukuta, N.: Nonsteady-State Kinetics of Droplet Growth in Cloud Physics, Journal of the Atmospheric Sciences, 31, 1334–1343, https://doi.org/10.1175/1520-0469(1974)031<1334:NSKODG>2.0.CO;2, 1974.

Ormières, D. and Provansal, M.: Transition to Turbulence in the Wake of a Sphere, Physical Review Letters, pp. 6–9, https://doi.org/10.1103/PhysRevLett.83.80, 1999.

Passarelli, R. E.: Theoretical and Observational Study of Snow-Size Spectra and Snowflake Aggregation Efficiencies, Journal of the Atmospheric Sciences, 35, 882–889, https://doi.org/10.1175/1520-0469(1978)035<0882:TAOSOS>2.0.CO;2, 1978.

Patade, S., Prabha, T. V., Axisa, D., Gayatri, K., and Heymsfield, A.: Particle Size Distribution Properties in Mixed-Phase Monsoon Clouds from in Situ Measurements during CAIPEEX, Journal of Geophysical Research: Atmospheres, 120, 10,418–10,440, https://doi.org/10.1002/2015JD023375, 2015.

Patera, A. T.: A Spectral Element Method for Fluid Dynamics: Laminar Flow in a Channel Expansion, Journal of Computational Physics, 54, 468–488, https://doi.org/10.1016/0021-9991(84)90128-1, 1984.

Prabhakaran, P., Weiss, S., Krekhov, A., Pumir, A., and Bodenschatz, E.: Can Hail and Rain Nucleate Cloud Droplets?, Physical Review Letters, 119, 128 701, https://doi.org/10.1103/PhysRevLett.119.128701, 2017.

Prabhakaran, P., Kinney, G., Cantrell, W., Shaw, R. A., and Bodenschatz, E.: Ice Nucleation in the Wake of Warm Hydrometeors, arXiv:1906.06129 [physics], 2019.

Prabhakaran, P., Kinney, G., Cantrell, W., Shaw, R. A., and Bodenschatz, E.: High Supersaturation in the Wake of Falling Hydrometeors: Implications for Cloud Invigoration and Ice Nucleation, Geophysical Research Letters, 47, e2020GL088 055, https://doi.org/10.1029/2020GL088055, 2020.

Pruppacher, H. R. and Klett, J. D.: Microphysics of Clouds and Precipitation, Springer Netherlands, https://doi.org/10.1007/978-0-306-48100-0, 2010.

Rangno, A. L. and Hobbs, P. V.: Ice Particle Concentrations and Precipitation Development in Small Polar Maritime Cumuliform Clouds, Quarterly Journal of the Royal Meteorological Society, 117, 207–241, https://doi.org/10.1002/qj.49711749710, 1991.

Rønquist, E. M.: Optimal Spectral Element Methods for the Unsteady Three-Dimensional Incompressible Navier-Stokes Equations, Ph.D. thesis, Massachusetts Institute of Technology, 1988.

Schaller, R. C. and Fukuta, N.: Ice Nucleation by Aerosol Particles: Experimental Studies Using a Wedge-Shaped Ice Thermal Diffusion Chamber, Journal of the Atmospheric Sciences, 36, 1788–1802, https://doi.org/10.1175/1520-0469(1979)036<1788:INBAPE>2.0.CO;2, 1979.

Schiller, L. and Naumann, A.: Über Die Grundlegenden Berechnungen Bei Der Schwerkraftaufbereitung, Z. Ver. Dtsch. Ing, 77, 318–320, 1933.

Takahashi, T., Nagao, Y., and Kushiyama, Y.: Possible High Ice Particle Production during Graupel–Graupel Collisions, Journal of the Atmospheric Sciences, 52, 4523–4527, https://doi.org/10.1175/1520-0469(1995)052<4523:PHIPPD>2.0.CO;2, 1995.

Vardiman, L.: The Generation of Secondary Ice Particles in Clouds by Crystal–Crystal Collision, Journal of the Atmospheric Sciences, 35, 2168–2180, https://doi.org/10.1175/1520-0469(1978)035<2168:TGOSIP>2.0.CO;2, 1978.

Zhou, W. and Dušek, J.: Chaotic States and Order in the Chaos of the Paths of Freely Falling and Ascending Spheres, International Journal of Multiphase Flow, 75, 205–223, https://doi.org/10.1016/j.ijmultiphaseflow.2015.05.010, 2015.

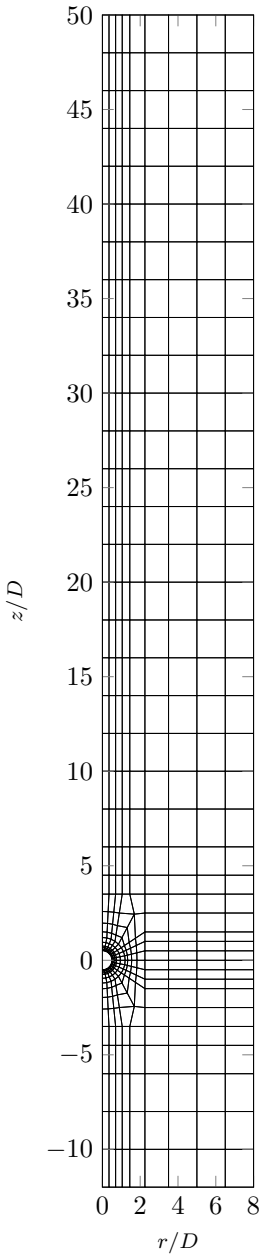

Figure 1. Spectral-element mesh in the axial-radial plane, where the lines depict the boundaries of the 463 elements. Each element contains $[6 \times 6]$ collocation points. The three-dimensionality is introduced by Fourier expansion in the azimuthal direction, which is truncated at the 7th Fourier mode, resulting in a cylindrical domain. A uniform velocity profile with constant temperature and vapor content is imposed at the upstream boundary, while the downstream boundary is subject to zero-gradient BCs for both velocity and scalars. The lateral boundaries are stress-free at zero pressure with zero-gradient BCs for the scalars. The surface of the spherical particle, whose center is located at the origin of the coordinate system, is impermeable and a no-slip BC for velocity is imposed as well as constant Dirichlet BCs for the scalar fields.

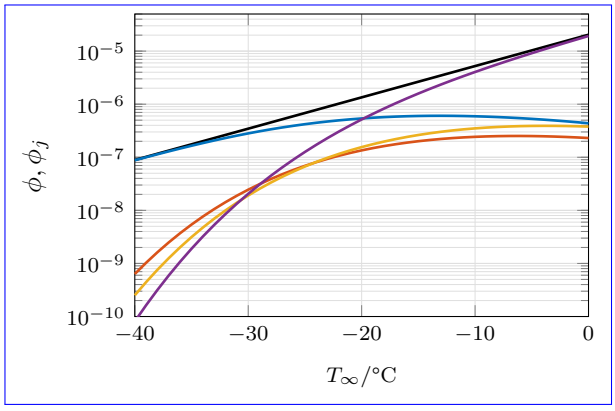

Figure 2. Volume fraction of ice particles in clouds as a function of ambient temperature. The total volume fraction ϕ is displayed by a solid black line (—), while the contribution by the regimes is given by the colored lines. Linestyles: axisymmetric regime (—), steady oblique regime (—), oscillating oblique regime (—), chaotic regime (—).

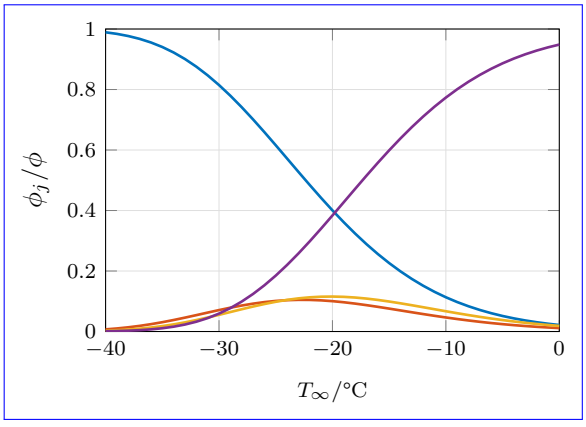

Figure 3. Relative contribution to the total volume fraction by hydrometeors in a certain regime. Linestyles: axisymmetric regime (—), steady oblique regime (—), oscillating oblique regime (—), chaotic regime (—).

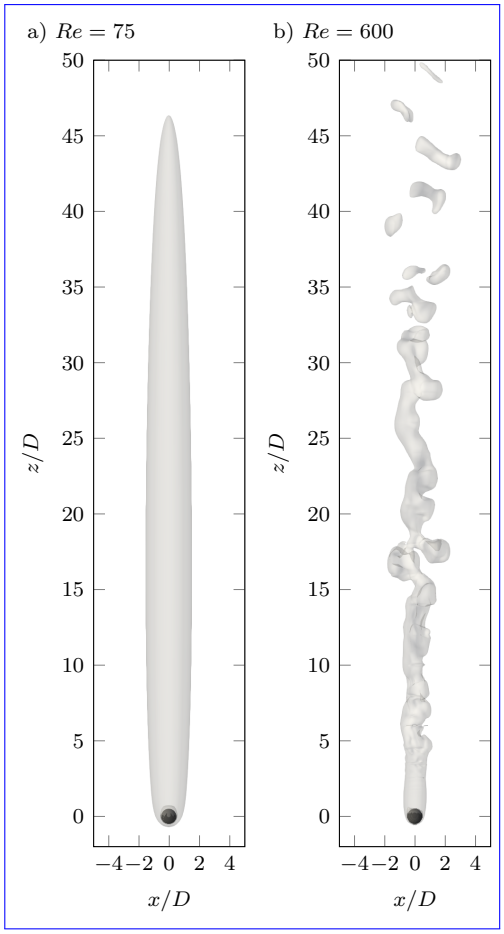

Figure 4. Isosurfaces of supersaturation in the wake at ~~$T_\infty = -30°C$~~$T_\infty = -15°C$. The value of the isocontour is ~~$\tilde{s}_i^* = 0.1$~~$s_{i,\infty} + 0.02$, i.e. ~~ten~~ two percentage points higher than the ambient supersaturation. Two different wake regimes are depicted, which correspond to two different hydrometeor sizes in our framework. (a) axisymmetric regime at $Re = 75$, (b) chaotic regime at $Re = 600$.

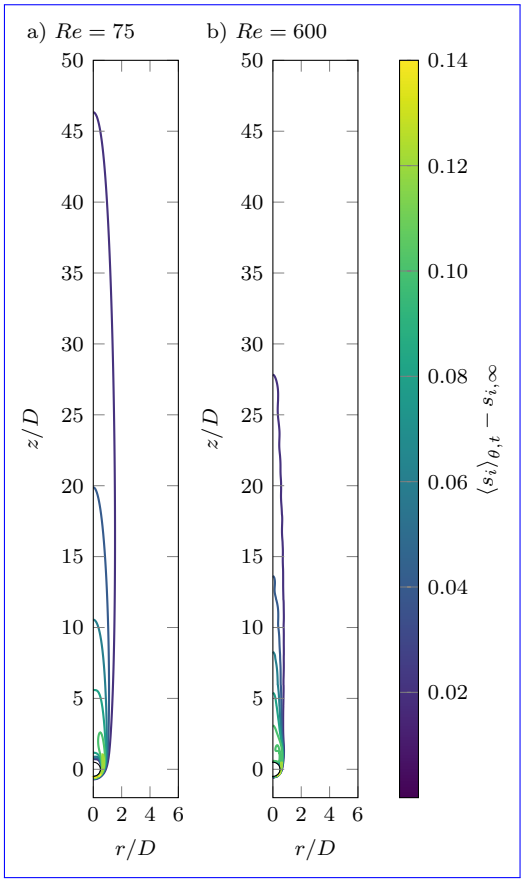

Figure 5. Contours of excess supersaturation in the wake, averaged over time and azimuthal direction at ~~$T_\infty = -30°C$~~$T_\infty = -15°C$. (a) axisymmetric regime at $Re = 75$, (b) chaotic regime at $Re = 600$.

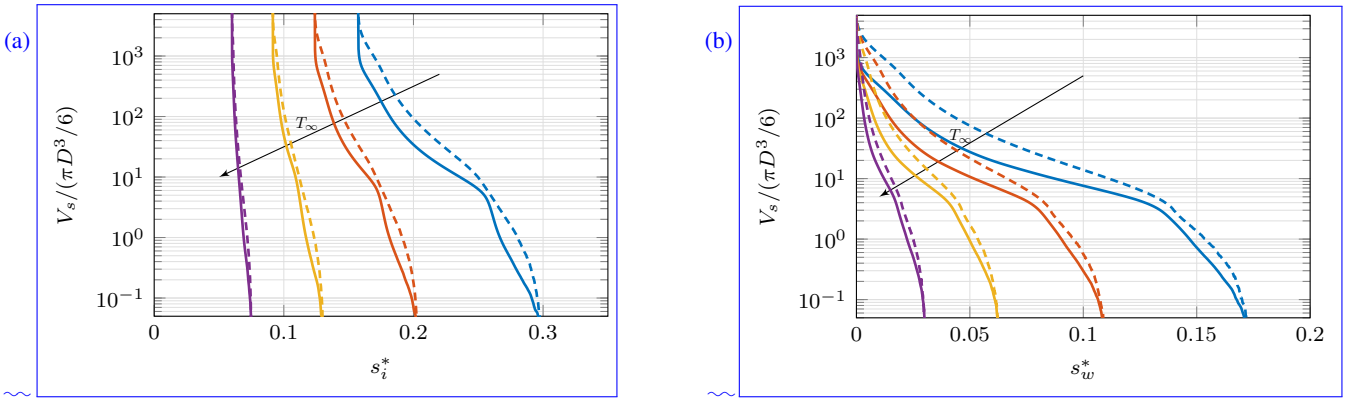

Figure 6. Volume of air where supersaturation exceeds a given threshold as a function of the threshold. The volume supersaturated w.r.t. to the solid phase is ~~normalized by~~ shown in (a), whereas (b) shows the volume supsaturated w.r.t. the liquid phase. The volume of the ice particle is used for normalization and ~~three~~ four different ambient temperatures are shown: ~~$T_\infty = -20°C$~~ $T_\infty = -6°C$ (——), ~~$T_\infty = -30°C$~~ $T_\infty = -9°C$ (——), ~~$T_\infty = -40°C$~~ $T_\infty = -12°C$ (——). $T_\infty = -15°C$ (——). Solid lines correspond to $Re = 600$ (chaotic regime, time average), while dashed lines show the data obtained for $Re = 75$ (axisymmetric regime).

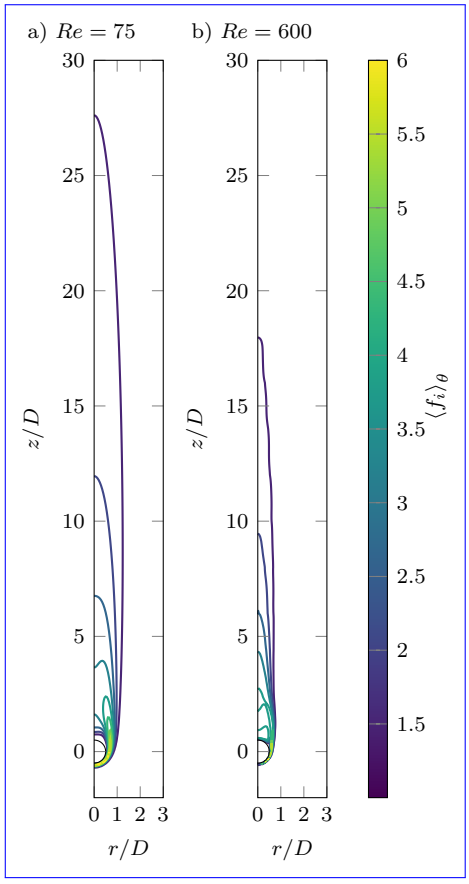

Figure 7. Contours of local ice enhancement factor in the wake, averaged over time and azimuthal direction at ~~$T_\infty = -30°C$~~$T_\infty = -15°C$. ~~The contour lines are spaced logarithmically.~~ (a) axisymmetric regime at $Re = 75$, (b) chaotic regime at $Re = 600$.

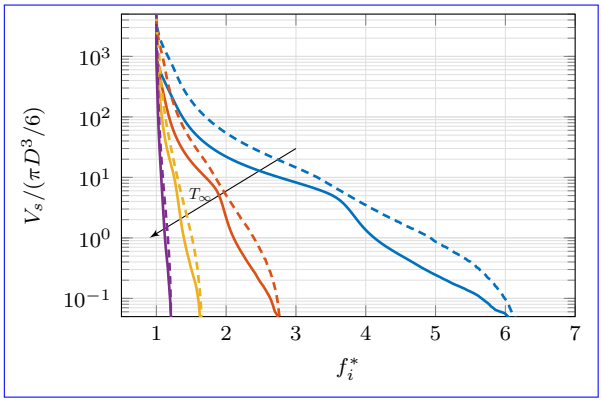

Figure 8. Volume of air with supersaturation above a given threshold as a function of the ice enhancement factor~~at $\alpha = 8$~~. The volume is normalized by the volume of the ice particle and ~~three~~ four different temperatures are shown: ~~$T_\infty = -20$°C~~ $T_\infty = -6$°C (——), ~~$T_\infty = -30$°C~~ $T_\infty = -9$°C (——), ~~$T_\infty = -40$°C~~ $T_\infty = -12$°C (——). $T_\infty = -15$°C (——). Solid lines correspond to $Re = 600$ (chaotic regime, time average), while dashed lines show the data obtained for $Re = 75$ (axisymmetric regime).

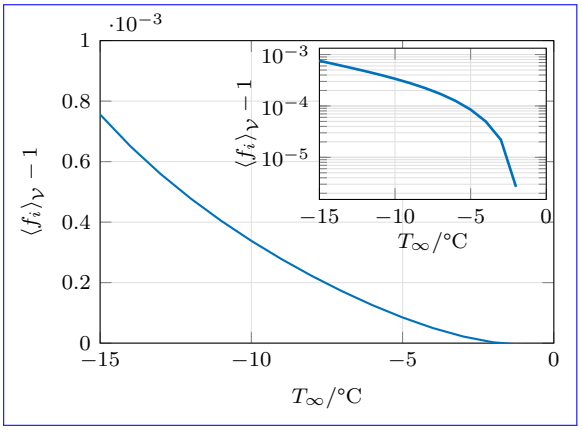

Figure 9. Global ice enhancement factor as a function of cloud temperature~~for various values of α~~. The inset shows the same data, but in semi-logarithmic scale. ~~Linestyles: $\alpha = 3$ (), $\alpha = 4$ (), $\alpha = 5$ (), $\alpha = 6$ (), $\alpha = 7$ (), $\alpha = 8$ ().~~

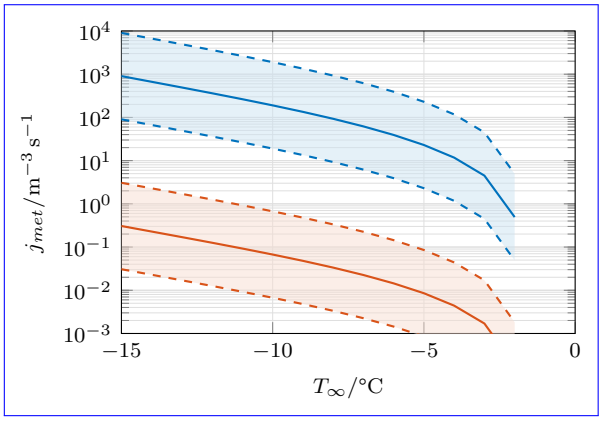

Figure 10. Limiting cases for the nucleation rate j_{met}. The swept-volume limited estimate based on the arguments of Prabhakaran et al. (2020) and evaluated from the present data according to Eq. (27) is shown for $C_{expo} = 10$ (——) with the shaded area depicting the values obtained for $1 < C_{expo} < 100$. The exposure-time limited estimate defined in Eq. (29), which is directly linked to the ice enhancement factor, is shown for $\tau_{nucl} = 10\mathrm{s}$ (——) and the range $1\mathrm{s} < \tau_{nucl} < 100\mathrm{s}$ (shaded area).